Characterization of the distribution of internal motions in the basic pancreatic trypsin inhibitor using a large number of internal NMR probes

GERHARD WAGNER

Institut für Molekularbiologie und Biophysik, Eidgenössische Technische Hochschule ETH-Hönggerberg, CH-8093 Zürich, Switzerland

I. INTRODUCTION

Proteins have a large variety of biological functions. For a large class of proteins the primary task is to react efficiently with other macromolecules or low molecular weight substances. In many cases these reactions involve motions and rearrangements of large protein moieties. Often the initial and final state, and perhaps an intermediate

one are known from X-ray crystallography. Very little is known, however, in most cases about the actual motions which are involved. Motions in small, non reacting proteins may be considered as model processes for reactions in larger systems. Moreover, internal motions are also certainly important for initiation of protein reactions or for degradation of proteins. It is therefore not surprising that internal motions in proteins *per se* have attracted much interest in enzymology, crystallography, spectroscopy and theory (see for example Austin *et al.* 1975; Careri, Fasella & Gratton, 1975; Wüthrich, 1976; Gurd & Rothgeb, 1979; Frauenfelder, Petsko & Tsernoglou, 1979; Artymiuk *et al.* 1979; Huber, 1979; Wüthrich & Wagner, 1979*a*; Karplus & McCammon, 1981*a*; Woodward, Simon & Tüchsen, 1982).

In this paper we summarize studies on internal motions in the basic pancreatic trypsin inhibitor (BPTI) using labile protons and aromatic side chains as internal NMR probes. BPTI has been chosen for these studies since it is available in large quantities, it has a low molecular weight (6500) but nevertheless has all the properties of a globular protein. Moreover, a very accurate crystal structure is available (Deisenhofer & Steigemann, 1975). The protein consists of a single polypeptide chain with three disulphide bonds. The regular secondary structures are a short 3_{10}-helix at the N-terminus, an antiparallel β-sheet involving the residues 16 to 35 which has a short third strand added by hydrogen bonds connecting the residues 21 and 45, and a short α-helix between the residues 47–56. A feature of particular interest is the enclosure of four water molecules with defined hydrogen bonds to polar groups of the polypeptide strand (Deisenhofer & Steigemann, 1975). Denaturation and folding of the protein have been studied extensively (Vincent, Chicheportiche & Lazdunski, 1971; Masson & Wüthrich, 1973; Creighton, 1978; Privalov, 1979; Wüthrich *et al.* 1980*b*; Jullien & Baldwin, 1981; Roder, 1981). In aqueous solution the denaturation temperature is above 90° between pH 3 and 8 (Privalov, 1979). At more extreme conditions of pH BPTI can be denatured by heat at lower temperatures. In the long term, however, irreversible denaturation occurs under these conditions, probably due to disulphide crosslinking and hydrolysis at high and low pH values, respectively. When studying internal motions in this globular protein we mainly concentrated on conditions far from denaturation so that essentially only fluctuations of the folded protein are examined. This does not exclude that denaturation-like fluctuations might also occur under these conditions. However, in this case they should be considered as a property of the dynamic protein conformation which can be described as a

dynamic ensemble of rapidly interconverting structural species (Wagner & Wüthrich, 1979b).

A structure as complex as a protein has many degrees of freedom, the number of which can be roughly estimated by the number of torsional angles. The state of lowest Gibbs free energy, G, could be characterized by a certain set of torsional angles $\{\phi_i^\circ, \psi_i^\circ, \xi_i^{j,\circ}\}$. A fluctuation of the protein structure involves a transient change in this set of torsional angles. Due to the many degrees of freedom a large number of fluctuations have to be expected; different in the lifetime, the frequency of occurrence or the size of the protein moiety involved.

To describe the spatial arrangement of a protein conformation in detail, a large number of experimental parameters has to be collected. In single crystals these data may be obtained by analysis of many reflexions in a scattering experiment. To characterize fluctuations of the spatial structure, the time dependence of the atomic coordinates or the torsional angles should be known for all the different internal motions. Up to now such information could not be obtained by an experimental technique. An indirect approach is to study internal motions by use of a large number of internal probes which are located at well-defined positions in the protein structure. These probes count the number of fluctuations which affect that site in the protein. In that way information about location of fluctuations, about the size of the protein moiety involved and about the mechanisms of the fluctuations can be obtained.

II. Detection of fluctuations by NMR-probes

Due to the high resolution of modern NMR instruments a large number of well resolved signals can be observed, each of which contains information about mobility at a particular spot in the protein structure. In this article we will concentrate only on two manifestations of internal motions in proteins: (i) the isotope exchange of labile protons which are manifested by changes in intensity with time for particular NMR signals, and (ii) the rotational motions of aromatic side chains which are manifested by line shapes and relaxation rates.

Labile protons and aromatic side chains are considered as internal probes which register internal motions of the protein. Since all the interior aromatic side chains of BPTI appear to be tightly packed between neighbouring groups in the crystal structure, rotational motions are only possible when fluctuations of the protein structure reduce the energy barriers which would oppose the rotational motions

in the equilibrium state. Interior labile protons which are completely shielded from solvent contact in the equilibrium conformation can exchange with the solvent only when fluctuations of the spatial structure provide solvent access to the protein interior or expose the interior labile proton.

(1) *Levels of information*

There are essentially two levels of information which can be obtained from experimental data on internal motions of proteins. The first level yields qualitative information obtained from a comparison of the measurable parameters of as many internal probes all over the protein as possible. From these data a topographical mapping of motions in the protein can be obtained. The second level of information concerns a physical understanding of the mechanism of probe recording, and the determination of quantitative parameters such as populations of activated states, the activation enthalpies, activation entropies or activation volumes, or the shape of energy barriers. This information may be obtained by variation of the experimental conditions, e.g. temperature or pressure. Since in a complex structure such as a protein many different fluctuations occur, the quantitative parameters obtained at the second level are average values because each internal probe is sampling over all the relevant fluctuations. Moreover, a change of experimental conditions will alter the distribution of fluctuations. Thus, when measuring at two different temperatures the sampling of the internal probes will be over different ensembles of fluctuations. This will sometimes inhibit the determination of quantitative parameters for the activated state.

(2) *Parameters of fluctuations*

For a fruitful discussion of fluctuations it appears to be necessary to define expressions which can be used to characterize the fluctuations. On this basis the necessary conditions for a probe to record a fluctuation can be discussed. We use $\{\mathbf{r}_i\}$ as the set of atomic coordinates of all the atoms i, and the dimensionless quantity $\rho(\mathbf{r})$ as the spatial distribution of the solvent which is one in the bulk solvent and o in the absence of solvent. A single fluctuation j shall be characterized by the change of atomic coordinates with time, $\{\mathbf{r}_i(t)\}_j$, when going from the equilibrium conformation, $\{\mathbf{r}_i^{\circ}\}$, to an activated state, $\{\mathbf{r}_i^{*}\}_j$, and back to the equilibrium conformation or a similar low energy state. The spatial distribution of the solvent will fluctuate in a complementary way, with $\rho_j(\mathbf{r}, t)$ describing the time dependence

of the solvent distribution during the fluctuation j. A more significant set of variables is the difference between the actual state and the equilibrium state,

$$\{\Delta \mathbf{r}_i(t)\}_j = \{\mathbf{r}_i(t) - \mathbf{r}_i^0\}_j, \tag{1}$$

and we denote the absolute values of these differences as

$$\{a_i(t)\}_j = \{|\Delta \mathbf{r}_i(t)|\}_j \tag{2}$$

and

$$\Delta \rho_j(\mathbf{r}, t) = \rho_j(\mathbf{r}, t) - \rho^0(\mathbf{r}, t), \tag{3}$$

and we denote the absolute value of this difference as

$$s_j(\mathbf{r}, t) = |\Delta \rho_j(\mathbf{r}, t)|. \tag{4}$$

Of particular interest are these parameters of the fluctuation j at the time t^*, when the system has reached the highest Gibbs free energy, G^*, and is supposed to be in the activated state. We define

$$a_{i(j)}^* = a_i(t^*)_{(j)} \tag{5}$$

as the individual amplitudes of the fluctuation j, and

$$A_j^* = \frac{1}{n} \sum_{i=1}^{n} a_{i(j)}^* \tag{6}$$

as the amplitude of the protein fluctuation j, and

$$S_j^* = \int s_j(\mathbf{r}, t^*) \, d\mathbf{r}$$

as the amplitude of the solvent fluctuation connected with the protein fluctuation j. For complete cooperative unfolding A_j^* will be of the order of the radius of gyration, R_G, and S_j^* will be of the order of the volume of the protein. The location of the fluctuation is defined by the subscripts, i, of the set $\{a_i(t^*)\}_j$ for which the $a_i(t^*)$ have sizeable values and by the spatial function $s_j(\mathbf{r}, t^*)$.

From the experiments described in this paper essentially two parameters can be derived. These are the rate at which the activated state is reached or the frequency of this event, denoted by k_1, and the life time of the activated state, denoted by k_2^{-1}. With individual assignments of the probes, information about location and amplitudes can further be derived.

(3) Necessary conditions for probe reactions

(a) Monomolecular probe reactions

We first discuss the conditions for reaction of an internal probe which does not need solvent contact for the reaction such as the flipping

motions of internal aromatic rings. For this reaction, (i) the location of the fluctuation has to overlap with the location of the probe, (ii) the individual amplitudes $a_{i(j)}^{*}$ at the site of the probe have to be comparable with the size of the probe, (iii) the lifetime of the fluctuation, k_2^{-1}, has to be comparable with or longer than some critical reaction time of the probe.

(b) *Reactions of probes with the solvent*

Conditions for successful isotope exchange of labile protons are: (i) the solvent has to reach the internal labile proton, (ii) the lifetime of the fluctuation has to be comparable with or longer than some critical reaction time of the probe.

(4) *Distribution of fluctuations*

If we have more than a single fluctuation we describe this situation by a distribution function. This can be represented as a distribution of amplitudes, A_j^{*} or S_j^{*}, a distribution of life times, k_{2j}^{-1}, a distribution of rates, k_{1j}, or a distribution of activation energies. The distribution will consist of discrete fluctuations. In the extreme case of many fluctuations this can be approximated by a pseudocontinuum representation, as shown in Fig. 1. In this figure we assume that large amplitudes are connected with large activation energies and use thus a Boltzmann distribution.

A certain probe records only those fluctuations which are located at the probe and have the necessary minimum amplitude. If the lifetimes of all the fluctuations are long compared to the critical reaction time of the probe, then all fluctuations with amplitudes larger than the minimum amplitude will be recorded by the probe. In Fig. 1 this is indicated by the step-shaped efficiency curve. For the rotational motions of the aromatic side chains the critical reaction time is determined essentially by the moment of inertia of the aromatic ring, and for the isotope exchange this quantity is given by the intrinsic exchange rates (see Englander, Downer & Teitelbaum, 1972). This estimation of the critical reaction times is valid, however, only for amplitudes of fluctuations much larger than the minimum necessary amplitude. For amplitudes around the critical value, frictional effects will increase the critical reaction times of the probes. Thus in this range of amplitudes the critical reaction time will depend on the amplitude of the fluctuation. This is pointed out with the broken efficiency curve in Fig. 1.

The experimentally measured parameters are obtained by the sampling of the probe over a subset of fluctuations of the distribution.
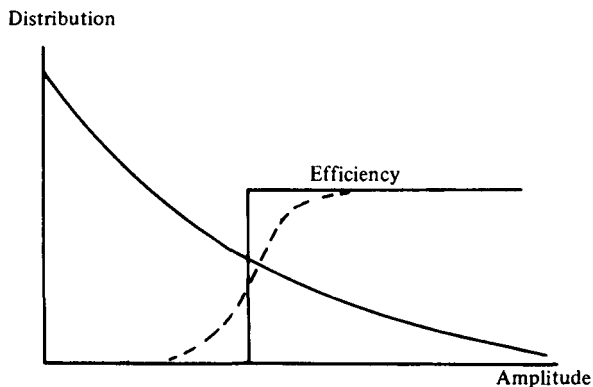
Distribution

Fig. 1. Schematic representation of a continuous distribution of fluctuations *v*. an amplitude. The efficiency of probe recording is given by the step function if the life time of the fluctuation is long compared with the characteristic time of probe reaction. If this is not the case the broken line is a characteristic efficiency curve. The sampling of the probe is obtained by the integral over the product of distribution function times efficiency.

The number of recordings of the probe is given by the integral over the product of the distribution function and the efficiency curve. This consideration shows that the sampling of the probe occurs over a limited class of fluctuations picked out around a critical amplitude which is approximately the minimum amplitude necessary for reaction of the probe. When the temperature or another external parameter is changed then the distribution of fluctuations will change. Moreover, the efficiency curve may change with temperature, pressure or pH. Thus the probe averages over a differently weighted subset of fluctuations. This will generally lead to non-linear Arrhenius plots or to non-standard pressure or pH-dependence. This is the case for a smooth continuous distribution as in Fig. 1. For a distribution of discrete classes of fluctuations it may be that at a certain temperature one class of fluctuations is dominant for the probe recording while at another temperature a different class of fluctuations dominates the recording of the probe. The main goal of the work described in this review is to get information about the shape of this distribution function.

III. THEORIES FOR RATE PROCESSES

When analysing internal motions in proteins one of the most significant parameters is the rate constant. To further rationalize this parameter,

often transition state theory is applied (Pelzer & Wigner, 1932; Eyring, 1935). In this theory we have for the rate constant, k,

$$k = \kappa \frac{{}^k B^T}{h} e^{-\Delta G^{\ddagger}/RT}, \tag{8}$$

κ is the transmission coefficient. In this theory the rate of crossing an energy barrier, $\Delta G^{\ddagger}$, is the product of the population of the activated state times the velocity on top of the barrier. The latter quantity is taken from a Maxwellian velocity distribution without consideration of interactions of the moving particle with its environment. Thus the system of the moving particle and its environment are treated as an entity, and frictional effects of the movement on the way to the activated state are transferred to an apparent activation energy, $\Delta G^{\ddagger}$, which thus might be different from the real energy difference between the activated state and the ground state, denoted by ΔG^*.

An alternative approach analyses the forces acting on a particle which is going to escape over a potential barrier. The forces are separated in a static and a time-dependent part, the first being a gradient of a potential, G, and the second a random force due to collisions with other particles:

$$\dot{p} = -\frac{\partial G(q)}{\partial q} + K(t). \tag{9}$$

p is the momentum and q the reaction coordinate.

Kramers (1940) has provided solutions for two limits of the Brownian motion. To obtain these solutions $K(t)$ is integrated over short time intervals, τ, which are sufficiently short that the momentum does not change during τ, but sufficiently long that $K(t)$ is uncorrelated with $K(t+\tau)$. This assumption means essentially that the time scales of the movements of the particles under investigation and that of the particles with which it collides are clearly separated. The integral

$$B_\tau = \int_t^{t+\tau} K(t')\, dt' \tag{10}$$

represents the momentum transferred by the collisions during the time τ. The average values of B_τ, B_τ^2, etc., are obtained by integration over a distribution function ϕ_B and yield expressions proportional to the friction coefficient, f.

$$\left. \begin{array}{l} \bar{B}_\tau = \displaystyle\int_{-\infty}^{+\infty} B_\tau \phi_B\, dB = -f\bar{p}\tau, \\[2mm] \overline{B_\tau^2} = \displaystyle\int_{-\infty}^{+\infty} B_\tau^2 \phi_B\, dB = 2f\overline{p^2}\tau. \end{array} \right\} \tag{11}$$

Using the equipartition theorem one obtains a relation between this second moment and the friction coefficient, f, independent of $\overline{p}$.

$$\overline{B_\tau^2} = 2k_B\,Tf. \tag{12}$$

The friction coefficient is proportional to the viscosity, η. Thus, the viscosity is an integral parameter representing the number and the average strength of these collisions. Low or high viscosity mean essentially few or many collisions, respectively. Using the moments $\overline{B_\tau^n}$ Kramers (1940) obtained

$$k = \eta\,.\,Ce^{-\Delta G^*/RT} \quad \text{for the low viscosity limit,}$$
and $\hspace{9cm}$ (13)
$$k = \frac{1}{\eta}\,.\,C'\,e^{-\Delta G^*/RT} \quad \text{for the high viscosity limit}$$

C and C' are constants which depend mainly on the shape of the potential function $G(q)$. In both limits the Arrhenius–Eyring type exponential factor is present where ΔG^* is the real difference in free energy between the activated state and the ground state. The net effect of the Brownian motion is given by the viscosity factor and is inverse in both limits. In contrast to the transition state theory the coupling between the reacting particle and the heat bath is now included explicitly. Concerning the rate of a process, the collisions by the Brownian motion have two effects. On the one hand they initially provide the kinetic energy to overcome the energy barrier, and on the other hand further collisions tend to stop the initialized motion. If the first effect is dominant we have the 'low-viscosity limit', if the second effect is dominant we have the 'high-viscosity limit'.

The assumptions concerning the parameter τ which Kramers used for integration of equation (9) are applicable only if the observed particles are much larger than their colliding counterparts. Thus these assumptions may not be appropriate for intramolecular processes in proteins where the moving protein moieties and the colliding counterparts have comparable size. Kramers' equations are strictly valid only if the random forces are δ-correlated and Guassian (Kubo, 1966).

$$\overline{K(t)\,K(t+\tau)} = k_B\,Tf\delta(\tau). \tag{14}$$

If this is not the case a frequency dependent friction coefficient, $f(\lambda)$, has to be used (Kubo, 1966). In this way modified Kramers' equations were derived for the high damping limit (Grote & Hynes, 1980):

$$k = \frac{C'}{\lambda + f(\lambda)/m}\,e^{-\Delta G^*/RT}, \tag{15}$$

λ is the frequency of the unstable reactive motion in the barrier region, and m the mass of the reacting particle. Transition state theory and the high viscosity limit of Kramers' theory are obtained from this equation for large and small λ, respectively. A corresponding treatment of the low viscosity limit of Kramers' theory is not yet available.

For analysis of data on internal motions in globular proteins neither the local viscosity is known nor is it obvious whether the low or the high viscosity limit prevails. When external parameters are varied, for example temperature or pressure, to obtain activation energies, activation entropies or activation volumes it has to be kept in mind that the local viscosity may also vary with these parameters. If we assume that the local viscosity of the protein interior behaves similar to that of normal hydrocarbon liquids we expect that η decreases with temperature and increases with pressure. If we further assume exponential behaviour we have:

$$\eta(T, P) = \eta_0 \, e^{+(E_\eta + PV_\eta)/RT}. \tag{16}$$

In the *low-viscosity limit* $\Delta H^\ddagger$ and $\Delta V^\ddagger$ obtained from transition state theory are therefore too small by E_η and V_η, respectively:

$$\left.\begin{aligned} \Delta H^\ddagger &= \Delta H^* - E_\eta, \\ \Delta V^\ddagger &= \Delta V^* - V_\eta. \end{aligned}\right\} \tag{17}$$

In the *high-viscosity limit* $\Delta H^\ddagger$ and $\Delta V^\ddagger$ are too large by the same quantities. To estimate the significance of $\Delta H^\ddagger$ or $\Delta V^\ddagger$ values obtained from transition state theory it is thus of importance to know whether the low- or high-viscosity limit prevails. This could be checked if the local internal viscosity could be varied to find out if the rate to be studied is proportional to η or to η^{-1}. Attempts have been made to change the internal viscosity by variation of the solvent viscosity. Some of these experiments will be discussed later in this paper.

IV. EXCHANGE OF LABILE PROTONS

One of the most characteristic features of a globular protein structure is the network of intramolecular hydrogen bonds. The difference in Gibbs free energy of intramolecular hydrogen bonds relative to intermolecular hydrogen bonds with the solvent is in the order of only a few kcal/mol. Thus opening and reforming of these bonds has to be expected to be a main feature of internal motions in proteins. As a consequence of the opening of hydrogen bonds, contact between

internal amide protons and the solvent may occur. Thus a study of isotope exchange of internal amide groups is an appropriate technique to investigate these phenomena.

(1) *Individual assignments of 58 labile protons*

BPTI consists of 58 amino acid residues. Since four residues are prolines we have 53 peptide bonds bearing labile amide protons which can be used to probe solvent accessibility and internal motions. In addition the side chain amide groups of three asparagines and one glutamine provide another eight NMR probes. The labile protons of arginine and lysine side chains can also be observed in the NMR spectra at low pH, but due to lack of resolution and because these groups seem to be mainly on the protein surface, they are not studied any further here.

The interpretation of the isotope exchange experiments depends crucially on the individual assignments of the resonances of the labile protons. The first three assignments of amide resonances were obtained by chemical modifications and the use of shift reagents with reference to the crystal structure (Marinetti, Snyder & Sykes, 1976). Later on Dubs, Wagner & Wüthrich (1979) have assigned 15 labile peptide protons and two labile protons of an asparagine side chain by spin decoupling and one-dimensional nuclear Overhauser enhancement (NOE) experiments. Finally two-dimensional NMR techniques led to an almost complete assignment of the ^{1}H NMR spectrum of BPTI without reference to the crystal structure (Nagayama & Wüthrich, 1981; Wagner, Anil Kumar & Wüthrich, 1981; Wagner & Wüthrich, 1982a). In particular all peptide amide protons were assigned except that of Gly 37. The $C^{\alpha}H_2$ resonances of the latter residue have been identified but the NH-$C^{\alpha}H_2$ cross peaks are not present in the two-dimensional correlated (COSY) spectra, perhaps due to some internal exchange reaction (Wagner & Wüthrich, 1982a). The assignment procedure was facilitated by the high resolving power of the two-dimensional NMR experiments at high magnetic field. This is demonstrated in Fig. 2 with a COSY spectrum of BPTI in H_2O solution. The normal one-dimensional spectrum appears on the diagonal. Off diagonal peaks indicate J-coupling between the corresponding resonances on the diagonal. Of particular interest are the cross peaks between peptide protons (6·5–11 ppm) and C^{α}-protons (1·5–6 ppm). This section of the spectrum is shown in Fig. 3 A in a contour plot representation. Only the part located above the diagonal in Fig. 2 is shown. In this spectral region each peptide proton is

BPTI in H_2O
COSY
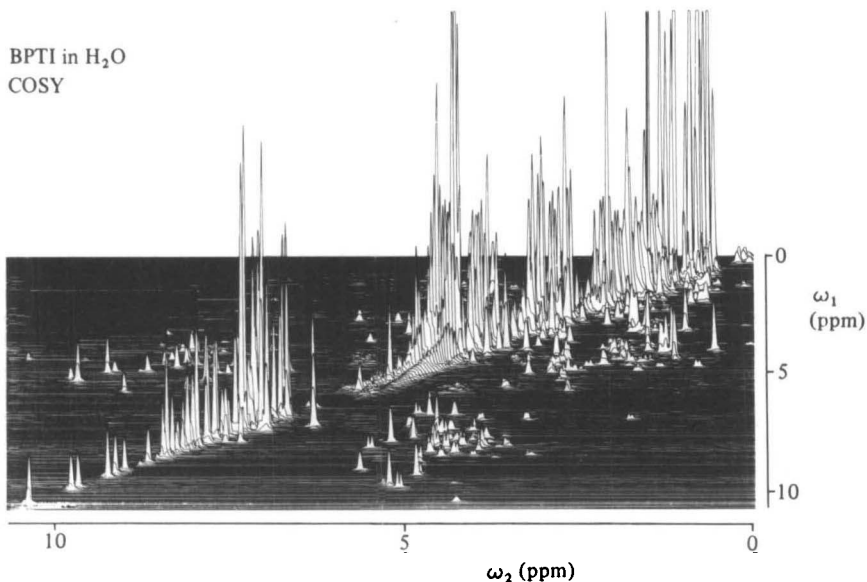
Fig. 2. Stacked-plot representation of a 500 MHz ^1H COSY (two-dimensional correlated spectroscopy) spectrum of a 0·02 M solution of BPTI in a mixed solvent of 90 % H_2O and 10 % ^2H_2O, pH 4·6, $T = 80$ °C. (Reproduced with permission from Wagner & Wüthrich (1982 a).)

represented by one signal except the glycines which show two peaks. Due to these individual assignments a complete set of single proton exchange rates may be obtained.

Two other techniques can provide hydrogen exchange data of individually assigned labile protons. Rosa & Richards (1979) have followed the tritium out-exchange in Ribonuclease S. Structural resolution was obtained by fast digestion and high pressure chromatography of partially exchanged samples. Thus single proton exchange rates were obtained for the S-peptide. Kossiakoff (1982) and Wlodawer & Sjölin (1982) have followed the hydrogen deuterium exchange in protein crystals by neutron diffraction techniques and obtained spatial resolution of exchange data. This technique is complementary to the 2-dimensional NMR technique since the data are obtained from crystals, and it would be very interesting to study the same protein with both techniques. Neutron diffraction has the advantage not to be restricted to low molecular weight proteins while the 2-dimensional NMR technique appears to be more versatile with respect to variation of pH, temperature, buffers or concentration.

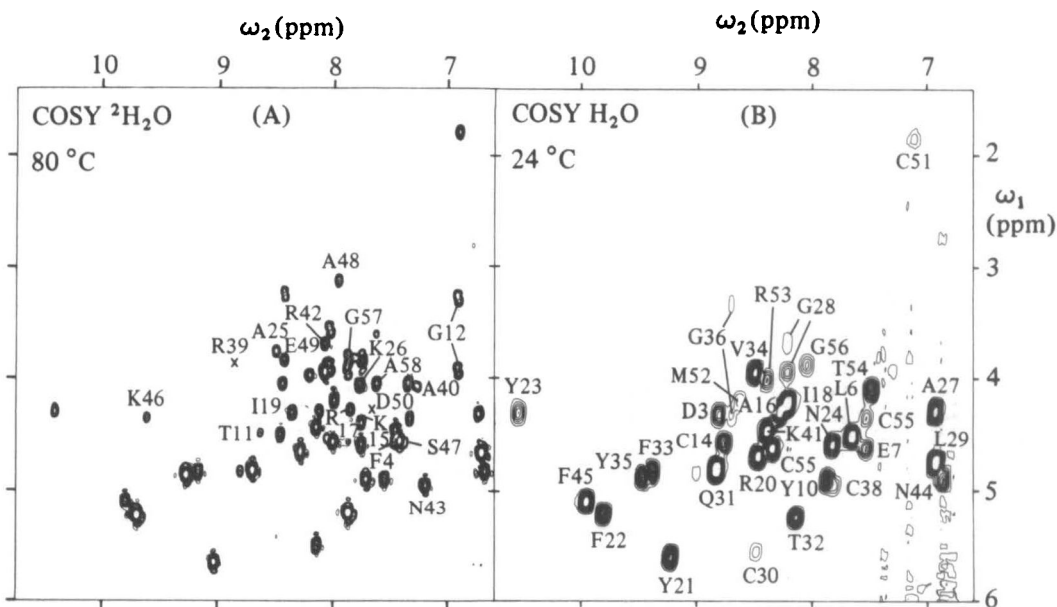Fig. 3. (A) Contour plot of the spectral region ($\omega_1 = 1\cdot5$–$6\cdot0$ ppm, $\omega_2 = 6\cdot6$–$10\cdot8$ ppm) of the COSY spectrum in Fig. 2. At the pH and temperature chosen for this experiment (see Fig. 2), this spectral region contains exclusively $C^\alpha H$–NH J-cross peaks. It thus presents a 'fingerprint' of the protein. The present spectrum contains the NH–$C^\alpha H$ cross peaks for 50 residues, and the peak locations for Arg 39 an Asp 50, which were for technical reasons observed in different experiments, are indicated by X. 52 of the 58 residues in BPTI are thus represented, i.e. all except Arg 1, Gly 37 and the 4 prolines. Individual assignments (Wagner & Wüthrich, 1982 a) to specific residues in the amino acid sequence are indicated for those 19 peaks which exchange too rapidly to be observed in spectrum B.

(B) Contour plot of the same spectral region as in A, taken from a 500 MHz ^{1}H COSY spectrum of a fresh $0\cdot02$ M solution of BPTI in ^2H_2O, p^2H $3\cdot5$, $T = 24\,^\circ$C. This figure presents a reduced fingerprint, i.e. the $C^\alpha H$–NH cross peaks are seen only for those residues for which the amide proton exchanges relatively slowly with the solvent. 33 peaks can be seen and the assignments are also indicated. (Reproduced from Wüthrich & Wagner, 1982). Peaks of four additional slowly exchanging peptide protons appear if the spectrum is recorded at 10° (Wagner & Wüthrich, 1982 b).

(2) *Solvent Accessibility in Solution and in the Crystal Structure*

When a protein is dissolved in ^2H_2O all the labile protons located on the protein surface, i.e. those which are accessible to the solvent, exchange within a few minutes with deuterium of the solvent. When a COSY experiment is carried out in ^2H_2O solution, the spectral region of the NH–$C^\alpha H$ crosspeaks (Fig. 3 B) contains only the solvent protected peptide protons. If the conditions for the experiment are chosen in a suitable way (Wagner & Wüthrich, 1982 b), a discrimination

between surface protons and interior protons is obtained. In Fig. 3 A all those peaks are identified which are only seen in H_2O solution and thus are assigned to surface protons. Fig. 3 B contains only signals from solvent protected parts of the protein. In Table 1 all surface protons are identified with an 'f' while for the solvent protected amides exchange rates are given. For details see Wagner & Wüthrich (1982 b). Previously Lee & Richards (1971) have introduced a method for probing X-ray structures for solvent accessibility. By computer modelling they move a sphere of the size of a water molecule over the surface and determine the accessible surface area of each residue and each atom of the protein. This kind of calculation has been carried out for BPTI by Chothia & Janin (1975) who provided us with detailed data (Chothia, private communication). In Table 1 and Fig. 4 we compare these data with the results of the NMR measurements. This comparison yields three classes of labile protons:

(1) For 42 of the 53 peptide protons the NMR data are in agreement with the X-ray data. This means that those labile protons which are accessible in the X-ray structure exchange rapidly in the NMR experiment, and those which are inaccessible according to the X-ray structure exchange slowly in solution.

(2) The amide proton of Glu 49 appears inaccessible in the crystal structure but exchanges rapidly in solution.

(3) The ten amide protons of Asp 3, Glu 7, Gly 12, Ala 16, Ala 25, Gly 28, Cys 30, Thr 32, Val 34 and Lys 41 are accessible in the crystal structure but exchange slowly in solution.

For four protons of the latter group (Asp 3, Cys 30, Thr 32 and Val 34) the unexpected slow exchange seems to be due to an aggregation. The exchange experiments were normally carried out at 20 mM protein concentration. When the exchange was measured in 0·2 mM solution none of these four protons showed slow exchange. The one labile proton which exchanges faster than expected from the crystal structure (Glu 49) forms a hydrogen bond to a carboxyl group of its own side chain (Wüthrich & Wagner, 1979 b). This hydrogen bond on the protein surface may not be stable enough to protect the amide proton from solvent contact. It may even catalize the exchange of the labile proton.

Thus a real discrepancy between solution structure and crystal structure exists for at most six out of 52 peptide groups which can be observed by this technique. This shows a gross similarity of the conformations in the crystal and in solution. The most remarkable discrepancy appears at the residue Glu 7. In the crystal structure a

distorted 3_{10}-helix is formed at the N-terminus, with two hydrogen bonds from Pro 2 to Cys 5, and from Asp 3 to Leu 6. Thus only the two amide protons of Cys 5 and Leu 6 would be involved in H-bonds. The observation that the amide proton of Glu 7 is also slowly exchanging could indicate that the helix proceeds up to this residue with a third H-bond between the carbonyl oxygen of Phe 4 and the NH of Glu 7.

Some additional information on intramolecular hydrogen bonds and salt bridges in solution can be obtained from pH-titration experiments. Since the pK_a values of all ionizable groups in BPTI

TABLE 1. *Rate constants k_m (in 10^{-3} min^{-1}, $\pm 10\%$) for the exchange of individual backbone amide protons in BPTI at p^2H 3·5 and 36 °C and 68 °C*

(For 68 °C and p^2H 3·5 the intrinsic exchange rates, k_3 are also given. Further, the following properties of the individual amide protons in the crystal structure of BPTI are listed: Accessible surface area and hydrogen bonding (adapted from Wagner & Wüthrich, 1982b).)

| Amino acid residue | In solution | | | In the crystal | |
	k_m (36°)*	k_m (68°)*	k_3 (68°)†	Accessible surface area‡	Hydrogen bonding§
Arg 1	n.o.	n.o.	—	27·5	—
Asp 3	10	~330	37000	4·6	—
Phe 4	f	f	51000	2·5	—
Cys 5	1·9	93	110000	0·0	3_{10}
Leu 6	0·31	23	56000	0·0	3_{10}
Glu 7	0·28	14	39000	1·0	—
Tyr 10	1·2	93	24000	0·0	W
Thr 11	f	f	39000	3·2	—
Gly 12	~100	f	40000	3·3	—
Cys 14	1·1	230	88000	0·0	W
Lys 15	f	f	69000	4·0	—
Ala 16	1·5	87	56000	1·6	β
Arg 17	f	f	35000	4·8	—
Ile 18	0·0022	6·5	56000	0·0	β
Ile 19	f	f	30000	3·6	—
Arg 20	<0·0004	7·1	35000	0·0	β
Tyr 21	<0·0004	5·6	44000	0·0	β
Phe 22	<0·0004	5·9	28000	0·0	β
Tyr 23	<0·0004	6·2	28000	0·0	S
Asn 24	0·00049	12	88000	0·0	β
Ala 25	~100	f	78000	1·8	—
Lys 26	f	f	35000	0·5	—
Ala 27	~45	~320	56000	0·0	β
Gly 28	1·8	52	80000	0·4	β

TABLE 1 (cont.)

Amino acid residue	In solution			In the crystal	
	k_m $(36°)$*	k_m $(68°)$*	k_3 $(68°)$†	Accessible surface area‡	Hydrogen bonding§
Leu 29	0·011	9·6	59000	0·0	—
Cys 30	∼80	f	88000	1·0	—
Gln 31	0·00048	11	78000	0·0	β
Thr 32	4·3	210	123000	3·6	—
Phe 33	0·0010	6·8	44000	0·0	β
Val 34	3·1	140	36000	4·6	—
Tyr 35	0·0044	10	24000	0·0	β
Gly 36	0·070	50	99000	0·0	β
Gly 37	n.o.	n.o.	158000	0·0	—
Cys 38	∼80	f	175000	0·0	S,W
Arg 39	f	f	69000	7·2	—
Ala 40	f	f	56000	2·6	—
Lys 41	0·51	180	35000	0·2	W
Arg 42	f	f	70000	1·8	—
Asn 43	∼100	f	139000	0·0	S
Asn 44	0·0075	37	196000	0·0	2₇
Phe 45	0·0013	20	62000	0·0	β
Lys 46	f	f	37000	2·4	—
Ser 47	∼100	f	174000	0·0	—
Ala 48	f	f	56000	0·7	—
Glu 49	f	f	39000	0·0	S
Asp 50	∼100	f	72000	0·0	S
Cys 51	0·22	∼50	144000	0·0	α
Met 52	0·057	11	56000	0·0	α
Arg 53	0·071	16	35000	0·0	α
Thr 54	0·49	33	174000	0·0	α
Cys 55	0·036	20	174000	0·0	α
Gly 56	2·1	79	156000	0·0	α
Gly 57	f	f	158000	3·0	—
Ala 58	f	f	63000	11·7	—

* The numbers give k_m in 10^{-3} min^{-1} ± 10 %. The sign ∼ in front of a number indicates that less than four experimental points were measured and therefore no error analysis was warranted. n.o., 'not observed', indicates that the NH resonance of this residue could not be detected in the COSY spectrum. f indicates that the amide proton exchanged too rapidly to be seen in the COSY spectrum recorded at 10 °C (see text). The following limits for the exchange rates of these protons were estimated: k_m $(36°) > 0·1$ min^{-1}; k_m $(68°) > 5$ min^{-1} (see Wagner & Wüthrich, 1982b).

† Intrinsic rate constants at p²H 3·5, which reflect inductive effects of neighbouring residues, were calculated according to the rules of Molday et al. (1972), starting from equation (2) of Englander et al. (1972). To obtain these data, pK_a values of 3·4, 3·8, 3·8, 3·0 and 2·9 were used for Asp 3, Glu 7, Glu 49, Asp 50 and the C-terminal Ala 58, respectively (Wüthrich & Wagner, 1979b). k_3 $(68°)$ in 10^{-3} min^{-1}.

‡ Accessible surface area in Å² as defined by Lee & Richards (1970). The calculations for BPTI are described in Chothia & Janin (1975). The data used here are taken from this reference and from a complete listing of the solvent accessibilities for all the atoms in BPTI which was kindly given to us by Dr C. Chothia.

§ 3_{10}, β, α and 2_7 indicate involvement in 3_{10}-helix, β-sheet, α-helix and 2_7-ribbon, respectively. S and W indicate hydrogen bonding to side chains and internal water molecules, respectively.
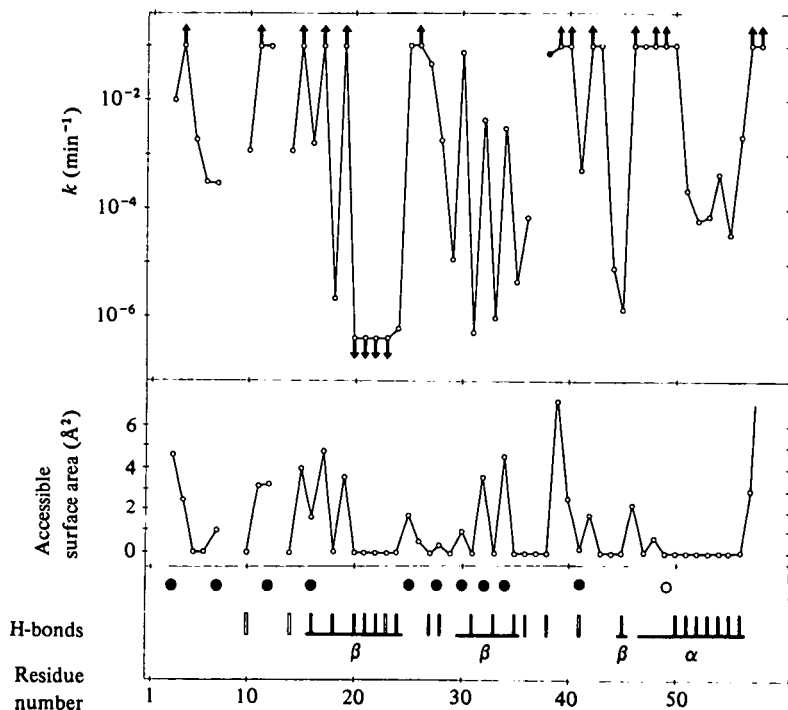
Fig. 4. Amide proton exchange data for BPTI at p^{2}H 3·5 and 36 °C and selected features of the crystal structure of BPTI. The horizontal scale represents the amino acid sequence of BPTI. The graph at the top is a logarithmic representation of the individual exchange rates, k_m, at 36 °C. Arrows pointing upwards indicate that the exchange was too fast to be observed with the COSY experiments. Arrows pointing downwards indicate that the exchange was too slow to be measured quantitatively within the maximum exchange time. In the lower part of the figure, the static accessible surface area is plotted for the backbone peptide nitrogens, and the intramolecular hydrogen bonds in the crystal structure of Deisenhofer & Steigemann (1975) are indicated by filled vertical bars (❙, intramolecular H-bonds with main chain carbonyls) or open bars (❚, H-bonds to side chains or internal water molecules). Residues which are part of regular α or β secondary structure are joined by horizontal bars. ○, The single residue that has zero accessible surface area and k_m (36°) > 0·1 min^{-1}, ●, residues with non-zero accessible surface area and k_m (36°) $\leqq$ 0·1 min^{-1}. (Reproduced from Wüthrich & Wagner, 1982.)

are known (Wüthrich & Wagner, 1979b), a strong downfield shift of the NH-resonance of Lys 46 with increasing pH at the pK_a of Asp 50 can only be explained by hydrogen bonding between these two groups (see resonance a in Wüthrich & Wagner, 1979b). In a similar way an interaction between the side chain of Glu 7 and the peptide NH of Asn 43, and between the peptide NH of Glu 49 and its own side chain are manifested in the NMR spectrum of the protein
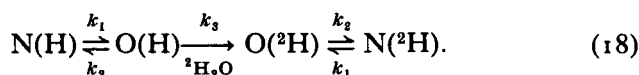
in solution (Wüthrich & Wagner, 1979b). Furthermore the existence of a salt bridge between the two termini was also established on the basis of pH-titrations (Brown *et al.* 1978).

(3) *Measurements of exchange rates in NMR spectra*

In one-dimensional NMR spectra the intensities of the absorption lines are directly proportional to the ^{1}H concentration at the respective peptide groups. This has commonly been used to measure exchange rates of well separated resonances. In two-dimensional correlated spectra the relative intensity of each cross peak is determined by the degree of protonation of the peptide group, by the J-coupling between NH and C^αH, and by the filter functions used for transformation. Therefore intensities between different cross peaks cannot be compared in hydrogen exchange experiments but the time dependence of the intensity of each individual cross peak can readily be used for determining exchange rates. Rather accurate rate constants could thus be obtained for all the interior amide protons (Table 1) (Wagner & Wüthrich, 1981b).

(4) *Mechanism of exchange of internal amide protons*

The exchange of internal amide protons can be described by the following equation (Hvidt & Nielsen, 1966):

$$N(H) \underset{k_2}{\overset{k_1}{\rightleftharpoons}} O(H) \xrightarrow[{}^2H_2O]{k_3} O(^2H) \underset{k_1}{\overset{k_2}{\rightleftharpoons}} N(^2H). \tag{18}$$

The closed state N(H) is in equilibrium with open states O(H). Exchange is possible only from the open states O(H) and leads, in the presence of ^2H_2O, to deuteration of the peptide site. The experimentally observable overall exchange rate k_m is approximately (Hvidt & Nielsen, 1966):

$$k_m = \frac{k_1 k_3}{k_2 + k_3}. \tag{19}$$

There are two limiting kinetic situations:

(a) EX_1 *process*

If $k_3 \gg k_2$ each opening of the closed state N leads to an isotope exchange and we have

$$k_m = k_1. \tag{20}$$

In this case the exchange rate gives directly the opening rate of the protein fluctuation. The p^{2}H- and temperature-dependences of the

protein fluctuations are directly obtained from k_m. If two amide protons are adjacent in the 3-dimensional structure of the protein and opening exposes both labile protons simultaneously, both protons should exchange in a correlated way. Correlated exchange implies, of course, equal exchange rates of adjacent protons, unless a local opening exposes only one of two adjacent protons.

(b) EX_2 process

If $k_3 \ll k_2$ only a small portion of all openings leads finally to the exchange of internal protons and

$$k_m = \frac{k_1}{k_2} k_3. \tag{21}$$

No correlated exchange would thus be expected for neighbouring protons. In this case the parameters of the protein fluctuations are masked by the intrinsic exchange rate k_3. Only if k_3 were known could the equilibrium constant k_1/k_2 be determined. The pH- and temperature-dependence of k_m contains contributions of k_1, k_2 and k_3. k_3 is directly proportional to the hydroxyl or hydronium ion concentration in the base or acid catalized regime, respectively. It has been measured in small model substances and is given by (see Englander *et al.* 1972):

$$k_3 = \frac{\ln 2}{200} (10^{pH-3} + 10^{3-pH}) . 10^{0.05 . T} \, min^{-1} \quad (T = temperature \, in \, °C). \tag{22}$$

Thus, in a plot of log k_3 $v.$ pH, it decreases with slope -1 below $p^2H \sim 3$ and increases with slope $+1$ above $p^2H \sim 3$. In the EX_2 process this pH-dependence should be contained in the experimentally observed exchange rate k_m.

(c) Experimental distinction of EX_1 and EX_2 in BPTI

The experimentally observed p^2H dependence of the exchange rates in BPTI indicates an EX_2 process. The rates decrease from p^2H 0 to p^2H 3 (acid catalysis) and increase again from p^2H 3 to p^2H 11 (base catalysis). This behaviour has been observed at different temperatures between 22° and 68° (Richarz *et al.* 1979; Hilton & Woodward, 1979). The appearance of a V-shaped curve for the p^2H dependence of the exchange rates is not a firm proof for EX_2 exchange. The criterium of the p^2H dependence fails if k_1 has by chance a similar p^2H dependence as k_3. A method has been proposed to distinguish EX_1 and EX_2 processes by nuclear Overhauser enhancement (NOE)
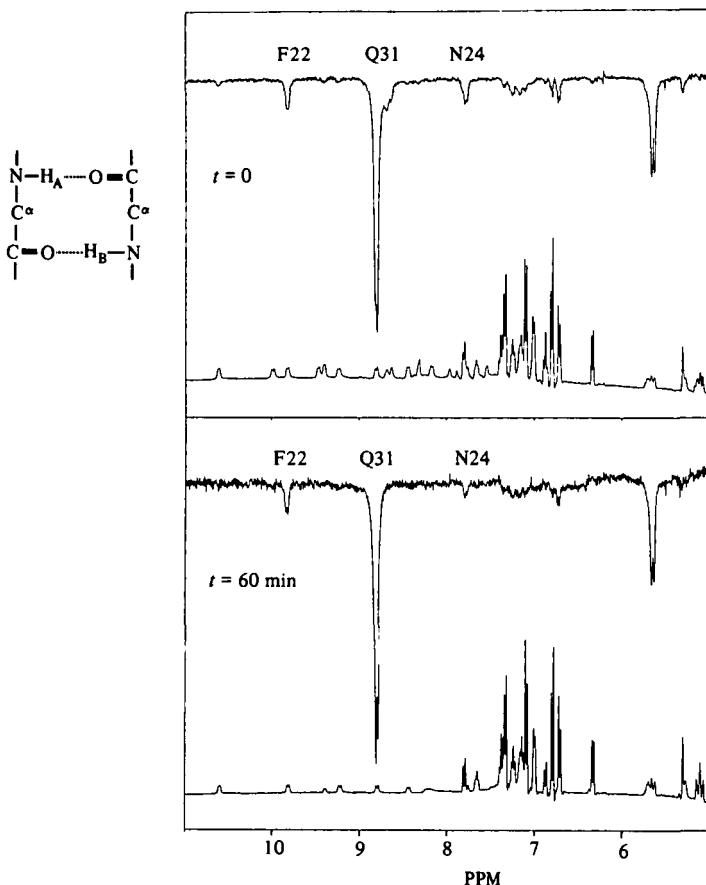
Fig. 5. Upper part: 360 MHz NOE differences spectrum (4000 scans) of a 20 mM solution of the basic pancreatic trypsin inhibitor in ^2H_2O at p^2H 4·6, 24 °C. Lower trace: reference spectrum; upper trace: NOE difference spectrum. Lower part: same experiment but prior to the measurement the sample was kept at 60°, p^2H 8·0 for one hour to partially exchange the amide protons. Left side: schematic representation of two adjacent hydrogen bonds connecting opposite strands of an antiparallel β-sheet. The two amide protons H_A and H_B are separated by approximately 2·6 Å. The relative magnetization transfer is the same in the fresh solution and in the partially exchanged sample (c. 12 %). This indicates correlated exchange at these conditions. (Reproduced from Wagner, 1980b.)

measurements between labile protons (Wagner, 1980b). This technique analyses the cross-relaxation between labile protons of close spatial proximity. This is demonstrated in Fig. 5. If two neighbouring protons exchange in a correlated way (EX_1) the apparent NOE between the two should be the same in a fresh solution and in a protein solution where the two peptide sites were half exchanged,

since either both sites are protonated or both are deuterated. In the uncorrelated case (EX_2) the NOE between the two labile protons should decrease with the exchange of the protons, since mixed pairs of protonated and deuterated peptide sites appear for which no ^1H–^1H NOE can be obtained.

(d) Selection of the dominant mechanism in a distribution of fluctuations

For a single fluctuation we have two characteristic parameters, the opening rate, k_1, and the lifetime of the fluctuation, k_2^{-1}. In a distribution of fluctuations which all provide EX_2-exchange the fluctuation with the largest value of k_1/k_2 appears as the dominant fluctuation. This will generally not be the most frequent fluctuation (with the largest k_1). For a given fluctuation a transition from exchange by EX_2 to exchange by EX_1 is expected to occur with increasing pH at conditions, where $k_3 = k_2$, since k_3 increases with pH while k_2 is constant. In a system with a continuous distribution of fluctuations with respect to the lifetime, k_2^{-1}, this transition may not be observable. This is readily apparent from the following considerations. When the fluctuation with the longest lifetime reaches the conditions of EX_1 exchange, its efficiency does not further increase with pH. Fluctuations with shorter lifetimes will thus become dominant. This will in general yield a slope < 1 in the plot of log k_m v. pH. On the other hand, when the distribution of fluctuations has discrete classes with respect to the lifetime, an EX_1 mechanism should be experimentally observable: When the fluctuations with long lifetimes have reached conditions of EX_1 exchange they remain the dominant mechanism for a certain pH interval, since the next class of fluctuations have a much shorter lifetime and become the dominant fluctuation only after a sizeable pH gap. Similar considerations apply for temperature variation, since closing rates of protein fluctuations appear to have a rather small temperature dependence (see, for example, Pohl, 1976) compared to the intrinsic exchange rates. Thus the experimental observation of EX_1 mechanism is a proof for the existence of discrete classes of fluctuations with respect to the lifetime.

(e) The intrinsic exchange rate k_3

The intrinsic exchange in a peptide group which is fully exposed to bulk solvent is assumed to consist of the following steps: diffusion of the solvent molecules which catalyse the exchange (H_2O, H_3O^+ or OH^-) to the peptide site, formation of hydrogen bonds between the

reacting particles, redistribution of hydrogen bonds and covalent bonds within the hydrogen bonded complex depending on the pK_a-values of the reacting groups, and finally dissociation of the hydrogen bonded complex and fast reactions with water which re-establish the original chemical situation (Eigen, 1964; Englander *et al.* 1972). Consistent with this mechanism equation (11) was experimentally established for small model peptides (Englander & Poulsen, 1969). Only acid and base catalysis was observed. No indication for general catalysis by H_2O was found for the exchange of peptide hydrogens. Molday, Englander & Kallen (1972) found that the exchange rates of peptide hydrogens are modulated by the neighbouring amino acid side chains which influence the pK_a-values of the peptide groups. The contributions of the two residues on both sides of the peptide group appear to be additive. With these data of Molday *et al.* (1972) the intrinsic exchange rates of fully solvent exposed polypeptide strands can be calculated.

For the case that a peptide group of a protein is not fully exposed to the bulk solvent it must be assumed that the diffusion of solvent molecules to the peptide site is somewhat hindered. In addition the pK_a-values of the peptide groups may be influenced by the anisotropic environment, and the rules of Molday *et al.* (1972) may not be applicable to this situation. This inhibits an accurate determination of kinetic parameters in the EX_2-exchange limit while an EX_1-exchange allows determination of a well defined single rate constant, k_1.

(5) *Change of experimental conditions*

Many different fluctuations appear to be relevant for the exchange of internal amide protons which have different characteristic parameters such as activation enthalpies, activation entropies or activation volumes. They may involve the opening of different H-bonds, salt bridges or van der Waals bonds. When experimental conditions, such as temperature, pressure or pH, are changed, a redistribution of the relative populations of the various fluctuations may occur (see Wagner & Wüthrich, 1979b). This will result in curved Arrhenius plots, in non-linear pressure dependence or in non-standard pH dependence for reaction rates. Moreover, a change of the exchange mechanism from EX_2 to EX_1 may occur, for example when going to high temperature or high pH.

(a) Change of mechanism with p^2H and temperature

Isotope exchange by EX_1 mechanism can be detected by observation
of correlated exchange of neighbouring protons. Correlated exchange
can usually be anticipated only under conditions where adjacent pro-
tons have similar exchange rates. In the β-sheet this is the case at high
temperatures and/or high pH. Three amide protons of the α-helix
(Met 52, Arg 53 and Cys 55) have similar exchange rates over a large
temperature range (Wagner & Wüthrich, 1982 b). NOE measurements
have shown that at p^2H 3·5 the exchange is uncorrelated up to 80°
for all regions of the BPTI structure (Wagner et al., to be published).
A systematic investigation of the protons of the β-sheet by Roder
(1981) has shown that at 68° the exchange is correlated between pH 7
and pH 10 while at lower or higher pH no correlation was observed.
At 45° no correlation could be observed in the whole pH range from
pH 3 to pH 11. Thus, when increasing the temperature at pH 8, a
transition from EX_2 to EX_1 occurs at about 50°. This transition with
increasing temperature can readily be understood, since fluctuations
with high activation enthalpies become more populated at high
temperature. It can be assumed that these fluctuations have larger
amplitudes and longer lifetimes, k_2^{-1}, than the fluctuations which are
relevant at low temperature since it takes more time to search for the
reclosing pathway of these large-amplitude fluctuations. Thus at
these temperatures the conditions for EX_1 exchange ($k_2 < k_3$) are met.
The pH dependence of the correlated exchange can be understood
along the same line of arguments. There are two classes of fluctuations
present which are relevant for the exchange of internal amide
protons: large amplitude fluctuations and small amplitude fluctuations
which have small and large refolding rates, respectively. At 68° and
low pH the large amplitude fluctuations may be less frequent (small
k_1) but more efficient than the small amplitude fluctuations if k_1/k_2
is larger due to the long lifetime, k_2^{-1}. Since k_3, the intrinsic exchange
rate, increases with pH, both types of fluctuations gain in efficiency
when pH is raised. Due to the longer lifetime, conditions of EX_1
exchange are obtained for the large-amplitude fluctuations at pH $\sim$ 7.
Thus $k_2 \approx k_3 \approx 10^3$ s^{-1} (see equation (22)) for the large-amplitude
fluctuations at 68°, pH 7. Thus with a further increase of pH the
efficiency of these fluctuations for isotope exchange does not increase
while the small amplitude fluctuations still gain in efficiency, since
they are still in the EX_2 limit. At around pH 10 the latter fluctuations
may become the dominant process for exchange and we observe

uncorrelated exchange up to pH 12. Thus, if k_3 can be estimated from equation 11, then $k_2 \gg k_3$ (68°, pH 12) $\approx 10^8 \text{ s}^{-1}$ for the small-amplitude fluctuations. This interpretation does not involve a redistribution of fluctuations with pH, it is just a kinetic switch due to the pH dependence of the intrinsic exchange rate k_3. Real physical changes of fluctuations with pH will be discussed below. At 45° the small-amplitude fluctuations seem to be dominant in the whole pH range and thus no transition to an EX_1 process can be observed. The observation of an EX_1 exchange indicates that there is a gap in the distribution of fluctuations v. lifetime, k_2^{-1}. This means we have discrete classes of fluctuations which are relevant for exchange in the β-sheet. Other molecular regions besides the β-sheet have not been investigated in this much detail due to problems of resolution which have only recently been overcome by the use of 2-dimensional NMR.

(b) *Variation of temperature*

The influence of temperature on the exchange rates has been studied for the amide protons which exchange most slowly by Richarz *et al.* (1979), Hilton & Woodward (1979), Woodward & Hilton (1980), and quite recently exchange rates at different temperatures were measured for the complete set of interior amide protons by 2-dimensional NMR (Wagner & Wüthrich, 1982*b*, Wagner *et al.*, to be published). For protons of the β-sheet, Woodward & Hilton (1980) have reported that the apparent activation energy, E_a, is ~ 60 kcal M^{-1} at p^2H 4·2 and 17–30 kcal M^{-1} at p^2H 9·5. At p^2H 8 they report a change of the slope of the Arrhenius plot at *c.* 40 °C, with an activation energy of ~ 60 kcal M^{-1} above 40 °C and a low-activation energy below 40 °C. They conclude that a change from a high-activation energy process to a low-activation energy process occurs with p^2H. In this interpretation it is not considered that the experimental data at p^2H 4·2 were recorded between 40° and 70°, the data at p^2H 9·5 between 24° and 33°, and the data at p^2H 8 between 24° and 60°. This selection of temperature ranges appears to be due to the p^2H dependence of the exchange rates. The rates can be measured conveniently, within reasonable time, at p^2H 4·2 only at high temperature, and at p^2H 9·5 only at low temperature. Thus the apparent change of the activation energy with p^2H, reported by Woodward & Hilton (1980), is in reality a temperature effect. These authors further did not consider that at p^2H 8 a change of mechanism from EX_2 to EX_1 occurs with temperature (Wagner, 1980*b*; Roder, 1981), since these data were not available at that time. Thus the apparent activation energy obtained

from the high temperature data at p^2H 8 is representative for the opening rate, k_1, while the apparent activation energy, E_a, measured at p^2H 4.2 is representative for the complex expression, $k_1 . k_3/k_2$. Thus the activation energies obtained at both conditions can not readily be compared. The values seem to be similar only by chance.

Recently we have measured the temperature dependence of all the slowly exchanging amide protons at p^2H 3.5 by 2-dimensional NMR (Wagner & Wüthrich, 1982b; Wagner *et al.*, to be published). At these conditions, where we have EX_2 mechanism up to 80°, the Arrhenius plots are curved for labile protons of all the interior regions of the protein, with the exception of Arg 20, Tyr 21, Phe 22 and Tyr 23. For these residues only an indication of a change in slope is seen at 46° while at lower temperature the exchange cannot be measured within a reasonable time (Wagner *et al.*, to be published). At high temperatures (70–80°), the apparent activation enthalpies, $\Delta H^{\ddagger}$, range from 85 kcal M^{-1} in the central β-sheet, over 75 kcal M^{-1} in the C-terminal α-helix to 60 kcal M^{-1} in the N-terminal 3_{10}-helix. At low temperatures (36–46°), a large spread of activation enthalpies is observed, with values of 30–40 kcal M^{-1} at the ends and the peripheral strands of the β-sheet, 13–19 kcal M^{-1} in the C-terminal α-helix, $\sim$ 18 kcal M^{-1} in the N-terminal 3_{10}-helix to values around 0 kcal M^{-1} in the turn of the β-sheet (Wagner *et al.*, to be published). These data indicate that a redistribution of fluctuations is obtained when the temperature is changed. At high temperature fluctuations with high activation enthalpies appear to dominate the exchange while at low temperature fluctuations with small activation enthalpies are relevant.

The apparent activation enthalpies, $\Delta H^{\ddagger}_{app}$, for the isotope exchange in the β-sheet, measured at p^2H 3.5 in our laboratory, are 20–30 kcal M^{-1} larger than the values measured at p^2H 4.2 by Woodward & Hilton (1980). This seems to be due to the different p^2H. Thus $\Delta H^{\ddagger}_{app}$ seems not to have a constant value in the range from p^2H 3 to p^2H 8 where large-amplitude fluctuations dominate the isotope exchange in the β-sheet. This indicates that a distribution of many fluctuations of somewhat different activation enthalpies constitute the ensemble of these large amplitude fluctuations, and a redistribution of these fluctuations seems to occur with p^2H (see Section IV. 4. d).

(c) *Variation of pressure*

The influence of pressure on isotope exchange in proteins has been studied up to now only by Carter, Knox & Rosenberg (1978), who

measured hydrogen–tritium exchange rates in lysozyme, ribonuclease A, oxidized ribonuclease A, and poly(DL-lysine). For the denatured protein and for poly(DL-lysine) a small increase of exchange rates with pressure was observed both, in the acid and base catalysed regimes. These data represent the pressure dependence of the intrinsic exchange rate, k_3. Since k_3 is proportional to the concentrations of ${}^2H^+$ or O^2H^-, respectively (see equation 22), the apparent activation volume, $\Delta V_{app}^{\ddagger}$, of k_3 can be separated into a contribution from the real chemical reaction and a second contribution from the pressure dependence of the dissociation constant of the water, K_W.

$$\Delta V_{k_3}^{\ddagger} = \Delta V_{chem.}^{\ddagger} + \Delta V_{K_W}. \tag{23}$$

The volume change for the dissociation of water, ΔV_{K_W}, is known to be $-20\cdot4$ ml M^{-1}. This appears to be the main contribution to $\Delta V_{k_3}^{\ddagger}$. From their experimental data, Carter *et al.* (1978) thus obtain a small positive activation volume, $\Delta V_{chem.}^{\ddagger}$, of $+6$ ml M^{-1} for the base catalysed reaction, and value of 0 ml m^{-1} for the acid catalysed reaction. The folded proteins were studied only in the base catalized regime, at pH $7\cdot0$. A slight increase of exchange rates was observed with pressure, with apparent activation volumes, $\Delta V^{\ddagger}$, of ~ -11 ml/M at 1 bar and ~ -25 ml/M at 2500 bar. Assuming an EX_2 mechanism, the activation volume for water dissociation was subtracted. Finally, for the base catalysed exchange at constant base concentration, a change of sign of the activation volume with increasing pressure was concluded, with $+9$ ml M^{-1} at 1 bar to -5 ml M^{-1} at 2500 bar. This observation was discussed as either an enhanced solvent penetration or an onset of reversible denaturation at high pressure.

Recently we have studied the pressure dependence of exchange rates of individually assigned protons in BPTI (Wagner, 1982; Wagner, to be published). Conditions of EX_1 exchange were chosen for the measurements (pH $8\cdot0$, 60°, see Wagner, 1980 b). One would then expect to measure the pressure dependence of the opening rate, k_1, alone. This would allow a more straightforward interpretation of the data than in the more complicated EX_2 situation. Fig. 6 shows, in a semilogarithmic plot, the complex results obtained from a pair of amide protons of the β-sheet, which is also typical for other protons of this molecular region (Wagner, to be published). At ambient pressure the rates of both protons are very similar, which is necessary for EX_1 exchange. Above 500 bar the rates start to become very different. This shows that above this pressure the exchange of these two protons is no longer correlated. Thus the mechanism switches
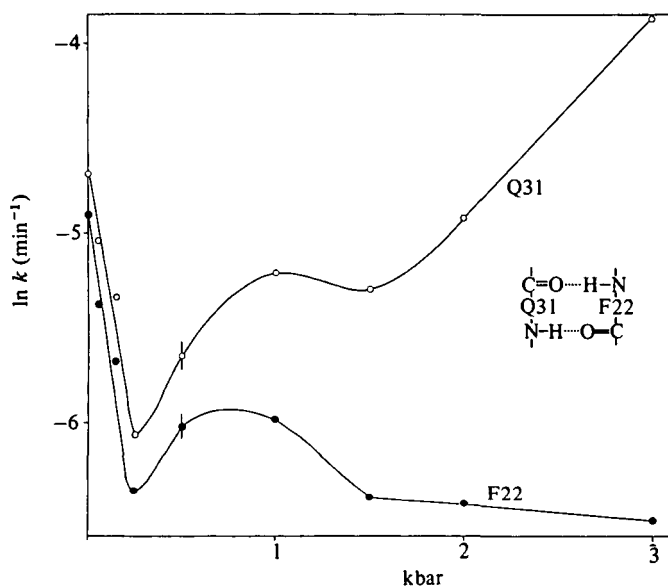
Fig. 6. Logarithm of the ^{1}H–^{2}H exchange rates for two adjacent amide protons of the β-sheet between 1 and 3000 bar at p^{2}H 8·0, 60°.

TABLE 2. *Apparent activation volumes*, $\Delta V^{\ddagger}_{\mathrm{app}}$, *for the exchange of some interior protons at pH* 8, 60°, *in the low-pressure limit* (EX_1 *exchange*)

$\Delta V^{\ddagger}_{\mathrm{app}}$ (Å³)	Residue
230	Arg 20
230	Tyr 21
250	Phe 22
250	Tyr 23
200	Asn 24
230	Gln 31
270	Phe 33
220	Phe 45
150	N$^{\delta}$ Asn 43

from EX_1 to EX_2 at ~ 500 bar. The apparent activation volumes, $\Delta V^{\ddagger}$, for the EX_1 process at low pressure are of the order of 250 Å³ for the residues of the central part of the β-sheet and somewhat smaller at Asn 24 and the side chain of Asn 43 (see Table 2). These values deviate from earlier data (Wagner, 1982) where only a smaller set of data was available, and the striking feature between 1 and 500 bar could not be detected. The large positive activation volumes

indicate that the activated state of the protein with its hydration shell is larger than the equilibrium state. Some contributions to the volume expansion of the activated state could be (i) a loosening of the structure which leads to an increase of the number and the size of packing defects, (ii) an increase of the solvent accessible surface area and thus an increase of the number of water molecules involved in the hydration layer. These water molecules cannot form as perfect hydrogen bonds as in bulk water and will therefore occupy more volume than in bulk water. The similar size of $\Delta V^{\ddagger}$ for all the protons of the central β-sheet indicates that this molecular region is exposed to bulk solvent simultaneously by the same class of large amplitude fluctuations. For the other parts of the β-sheet, i.e. Ile 18, Tyr 35, Ala 16, Asn 24 and the β-turn, additional fluctuations expose these protons since the activation volumes are smaller (Asn 24) and the rates are much faster than in the central part.

Above 250 bar small-amplitude fluctuations seem to become relevant for the exchange, similar to those which dominate the exchange at high pH or low temperature. The switch of exchange mechanism by pressure can not be attributed to a pH change since the CH_3 resonance of Ala 58 which is pH dependent at pH 8·0 (Brown *et al.* 1978) does not shift with pressure. A possible explanation would be the pressure dependence of the water dissociation constant. With increasing pressure the large amplitude fluctuations which exchange internal protons by an EX_1 mechanism, lose efficiency due to the large positive activation volume of k_1. Simultaneously the small-amplitude fluctuations, which provide exchange by an EX_2 process, gain in efficiency since the OH^--concentration increases due to the pressure enhanced dissociation of the water. Above $\sim$ 500 bar these fluctuations appear to become dominant for the exchange.

(d) *Variation of charge distribution*

The most convenient method for variation of the charge distribution in a protein is to change the pH. When interpreting the p^2H dependence of exchange rates, intrinsic effects such as the V-shaped p^2H profile in the EX_2-regime or the switch from EX_2 to EX_1 mechanism, have to be distinguished from real physical changes of the fluctuations with p^2H. A complete set of data is available for BPTI only for 9 residues of the β-sheet region (Ile 18, Arg 20, Tyr 21, Phe 22, Tyr 23, Gln 31, Phe 33, Tyr 35 and Phe 45) and for 3 residues of the α-helix (Met 52, Arg 53 and Cys 55), measured at 22° and 45° (Richarz *et al.* 1979), and for small p^2H ranges also at 68°, 51° and

33° (Hilton & Woodward, 1979). The striking features of these data are:

(1) the minima of the V-shaped p^2H profiles are generally much broader than for model peptides;

(2) For several residues the position of the minimum is shifted to higher pH, compared to model peptides;

(3) For three residues (Tyr 21, Phe 22 and Tyr 23) the slope in the base catalysed regime of the curve log k_m v. pH is very flat compared to model peptides.

The first two points can be understood from the titration of the carboxylate groups. It appears that the deprotonation of these groups with pK_a values between 2·9 and 3·8 (Wüthrich & Wagner, 1979b) stabilizes the closed states of the protein (see equation 7). Thus k_1/k_2 decreases with p^2H in the region of the pH of minimal exchange. As a result the minimum of the V-shaped p^2H profile is broadened and shifted to higher p^2H. It can therefore be concluded that upon deprotonation at least part of the carboxylic groups form salt bridges or hydrogen bonds which oppose the opening of the conformation (equation 7). From an inspection of the X-ray data, and from NMR pH titration experiments at least three such titrations can be identified: a salt bridge between the C-terminus and the N-terminus (Brown *et al.* 1978), a hydrogen bond between the side chain of Glu 7 and the peptide amide group of Asn 43 (Deisenhofer & Steigemann, 1975), and a hydrogen bond between the side chain of Asp 50 and the peptide amide group of Lys 46 (Wagner, unpublished result). The latter two interactions are in the immediate environment of the β-sheet structure, and it appears quite natural that they influence internal motions in that part of the molecule. It has further been shown that the salt bridge between C- and N-terminus stabilizes the β-sheet structure against internal motions since a removal of the charge at the N-terminus by transamination increases the isotope exchange rates in the whole β-sheet region (Brown *et al.* 1978).

The third striking feature of the p^2H-dependence is the small slope in the base catalysed regime for Tyr 21, Phe 22 and Tyr 23. This has been discussed by Wagner & Wüthrich (1979a, b) on the basis of a multistate model where the distribution of open states would be changed by the deprotonation of ionizeable groups. It is rather surprising that this phenomenon is only observed for the three residues located on the central strand of the triple stranded β-sheet while the residues of the peripheral strands, which are spacially close in the conformation show a quite normal slope (see Fig. 7). This
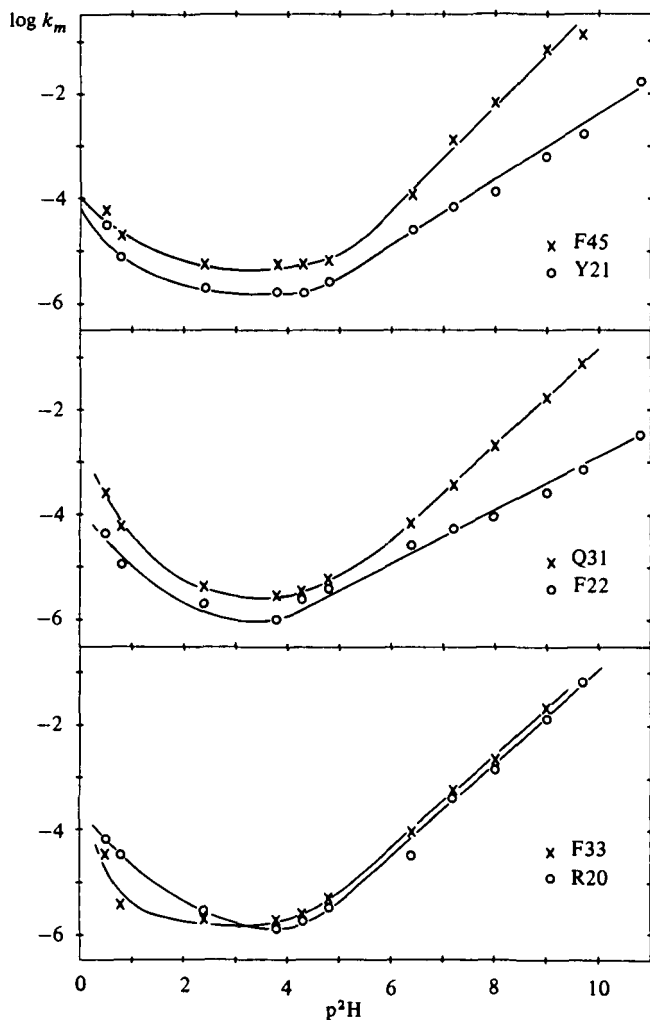
Fig. 7. p^2H dependence of the hydrogen exchange rates at $45°$ of two pairs of amide protons of the triple stranded β-sheet (Phe 45 and Tyr 21, Gln 31 and Phe 22) and one pair of the double stranded β-sheet (Phe 33 and Arg 20). (Data from Richarz *et al.* 1979.)

phenomenon may bear information which perhaps will lead to a better structural understanding of the internal motions involved.

In the α-helix the p^2H-dependence has been studied only for Met 52, Arg 53 and Cys 55 (Richarz *et al.* 1979). The data at $45°$ are shown in Fig. 8. It is striking that below pH $3\cdot5$ sizeable differences in the exchange rates occur while, above the p^2H the rates are almost identical for the three protons. This change of the exchange rates
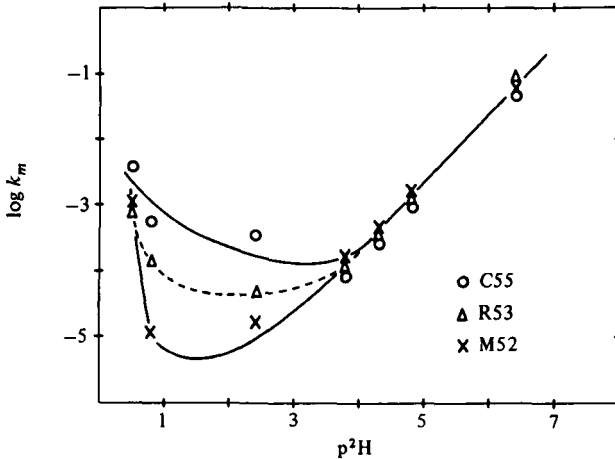
Fig. 8. Same as Fig. 7 for three residues of the α-helix.

coincides with the titration of the carboxylic acids. It may therefore be concluded that at least the interaction between the chain termini, and the hydrogen bond between Asp 50 and Lys 46 influence the fluctuations in the α-helix. It appears therefore that in the range where these carboxylates are negatively charged, the three amide protons are exposed only simultaneously by one type of fluctuation.

Another variation of charge distribution is obtained when homologous proteins are studied. In comparison with BPTI two other molecules were investigated for that purpose, i.e. a cow colostrum trypsin inhibitor and a trypsin inhibitor from *helix pomatia* (Wagner, Wüthrich & Tschesche, 1978 *a, b*). In both proteins Glu 7 and Asp 50 are replaced by non-acidic residues, and the location of the termini is shifted to other positions of the primary structure. Thus the three intramolecular interactions discussed above for BPTI cannot be present in these molecules. The exchange of internal amide protons of the β-sheet and the α-helix is much faster in both these proteins (Wagner *et al.* 1978 *a, b*). This indicates that the loss of the three intramolecular interactions destabilizes the protein with respect to those internal motions which are responsible for exchange of internal labile protons.

(6) *Mechanistic aspects*

The goal of hydrogen exchange measurements in proteins is to obtain insight into the spatial rearrangements of the protein conformation which lead to solvent contact and successful exchange of interior

labile protons. Three major classes of fluctuations have been discussed in the literature: solvent penetration, local unfolding and global cooperative unfolding (see, for example, Gurd & Rothgeb, 1979; Woodward, Simon & Tüchsen, 1982). A sharp distinction between these classes may be arbitrary since these three features just point out different degrees of opening of the folded protein conformation. Nevertheless these concepts are useful since they provide aspects which may be checked with the experimental data. A distinction between the three classes will be based on the size of the activation enthalpy and the observed p^2H dependence.

(a) Solvent penetration

When X-ray structures of globular proteins are studied, a number of small packing defects appear in the interior of the proteins. Lumry & Rosenberg (1975) have pointed out that transient rearrangements of these packing defects could create channel-like openings which might provide solvent access to the interior of the protein. It was then concluded that this channel-formation could be responsible for isotope exchange of interior amides. Richards (1979) has made an attempt to calculate quantitatively probabilities of channel formation. He estimated the mean square volume fluctuation for a protein of the volume, V, from the isothermal bulk compressibility, β_T (see Cooper, 1976).

$$\overline{\delta V^2} = kTV\beta_T. \tag{24}$$

This quantity was used to calculate the standard deviation, σ, of a normal distribution $p(n, v)$ that represents the probability to find n packing defects of volume v.

$$\sigma = \left(\frac{\overline{\delta V^2}}{n}\right)^{\frac{1}{2}}. \tag{25}$$

From this distribution Richards (1979) calculated the probabilities of formation of channels, reaching from the protein surface to the internal labile protons. The minimum size, v_0, of the volume of the elementary cells which constitute the channels was used as an adjustable parameter since it is not obvious what size is required to accommodate the species of solvent molecules which catalyse the exchange. Richards (1979) further assumed that the intrinsic exchange rate, k_3, within the channels would be similar to that of polyalanine in bulk solvent (see equation 22). This concept does not exclude the mechanism of partial unfolding. To obtain criteria for a distinction of solvent penetration and partial unfolding we further postulate that the major network of hydrogen bonds and most van der Waals

2

contacts are not opened during the process of solvent penetration. Thus, a ΔH of a few kcal/M is expected for this process. We further have to assume that, in long channels, the properties of the solvent, such as p^2H and the dissociation constant of the water, are determined by the local environment of the solvent in the channel rather than by the state of the bulk solvent. Thus for long channels the hydrogen exchange should not depend on p^2H.

In BPTI above 56°, at p^2H 3·5, all but two internal amide protons have activation enthalpies, $\Delta H^{\ddagger}$, larger than 30 kcal/M. Subtracting at most 17 kcal/M for the intrinsic exchange, the remaining ΔH is larger than 10 kcal/M. Further, an increase of exchange rates with p^2H is observed. These data indicate that, at these conditions, an opening process rather than solvent penetration dominates the exchange of these interior hydrogens.

BPTI has a particular property which may be used to further discuss if channel formation is an effective exchange mechanism. The protein contains a permanent enclosure of four water molecules (Deisenhofer & Steigemann, 1975). Three of these internal waters form hydrogen bonds with each other, and all but one have accessible surface areas > 0 Å^2 (Chothia, private communication). These internal waters are hydrogen bonded to the peptide hydrogens of Tyr 10, Cys 14 and Lys 41. In deuterated solvent these internal water molecules may be replaced very fast by ^2H_2O molecules since they have permanent solvent contact (compare Kossiakoff, 1982). Thus we have a natural permanent channel already in the closed protein conformation. In contrast to what we would expect for amides which are in permanent contact with the solvent, these three peptide hydrogens exchange very slowly (see Table 1). They have normal activation enthalpies, $\Delta H^{\ddagger}_{app}$, of 22, 44 and 46 kcal M^{-1}, respectively (at 60°, Wagner *et al.*, to be published) which is indicative for an opening process. From some preliminary experiments at different p^2H values it appears that a rather normal p^2H dependence exists, indicating base catalysis. These data indicate that for this particular region of the BPTI structure an opening mechanism is the relevant spatial fluctuation for these internal amide protons while the water channel does not promote hydrogen exchange, at least in the temperature range from 36 to 80°, at p^2H 3·5. Since this permanent water channel in BPTI does not promote hydrogen exchange it is unlikely that transiently created water channels of that type are relevant for hydrogen exchange, even if this channel formation were a frequent protein fluctuation.

At low temperature a number of amide protons that are located close to the protein surface have rather small activation enthalpies, even smaller than the 17 kcal/M of the intrinsic exchange rate, k_3 (Wagner *et al.*, to be published). For these protons solvent penetration might be considered as a possible exchange mechanism at low temperature.

The small-amplitude fluctuations which dominate the hydrogen exchange in the central β-sheet at very high p^2H (see Section 5 a) have larger activation enthalpies, $\Delta H^{\ddagger}$, of 17–38 kcal/M (Woodward & Hilton, 1980), and they show a normal increase of exchange rates with p^2H. Therefore these fluctuations seem to be partial unfolding rather than solvent penetration.

Further arguments for the solvent penetration mechanism originate from isotope exchange studies in protein crystals (Tüchsen, Hvidt & Ottesen, 1980). In these experiments the protein molecules were cross-linked in the crystals by formaldehyde treatment. This had the advantage that identical buffers could be used for isotope exchange in crystals and in solution. The exchange was followed by tritium tracer techniques. The data showed almost identical exchange curves in solution and in the cross-linked crystals and were interpreted in favour of the solvent penetration mechanism. Kossiakoff (1982) has studied hydrogen–deuterium exchange in trypsin crystals using neutron scattering. Due to his method he obtains spatially resolved data. He points out that a local unfolding mechanism would readily be possible in protein crystals while no evidence for exchange by channel formation was found in his data.

(b) Cooperative unfolding

A global cooperative unfolding of the conformation is certainly not a relevant fluctuation for hydrogen exchange for the great majority of internal labile protons in the whole temperature range up to 70° (at p^2H 3·5) since the exchange rates are very different for the individual protons. There remains to be investigated whether the innermost protons of the β-sheet exchange by a global cooperative unfolding. At 68°, p^2H 3·5, the amide protons of Ile 18, Arg 20, Tyr 21, Phe 22, Tyr 23, Asn 24, Leu 29, Gln 31, and Phe 33 have similar exchange rates (Wagner & Wüthrich, 1982b). The apparent activation enthalpies are between 77 and 88 kcal M^{-1} and do not change over the whole temperature range from 46° to 80°. The similarity of the exchange rates at these conditions might be taken to indicate that all the hydrogen bonds of the central β-sheet open

simultaneously at the fluctuations which propagate the hydrogen exchange in this molecular region. In order to check whether the open states obtained by these fluctuations could be identical with the states obtained by complete cooperative unfolding, we compare the equilibrium ΔH for the denaturation of BPTI with the activation enthalpy, $\Delta H^{\ddagger}$, of the hydrogen exchange. This is possible since in the EX_2-limit k_m is a product of an equilibrium constant, k_1/k_2, and the rate k_3 (see equation 21). Thus the activation enthalpy for the hydrogen exchange is a sum of an equilibrium enthalpy difference for the opening of the conformation, ΔH_{con}, and an activation enthalpy for the intrinsic exchange reaction, $\Delta H^{\ddagger}_{k_3}$:

$$\Delta H^{\ddagger} = \Delta H_{\mathrm{con}} + \Delta H^{\ddagger}_{k_3}.$$

$\Delta H^{\ddagger}_{k_3}$ is 17 kcal/M (Englander & Poulsen, 1969). Therefore the ΔH_{con} for the fluctuations of the β-sheet amounts to 60–70 kcal/M. These values should be compared with ΔH_d values for thermal denaturation. Privalov (1979) reported calorimetry data on the heat denaturation of BPTI, i.e. the pH dependence of the denaturation temperature, T_d, and of the enthalpy of denaturation, ΔH_d, in the range from pH 1·5 to pH 5. According to these data, ΔH_d would be 100 kcal/M at pH 3·5 at the denaturation temperature (97 °C). With a heat-capacity change, Δc_p, of 715 cal °K^{-1} M^{-1} (Privalov, 1979) we can extrapolate that ΔH_d would be approximately 88 kcal/M at 80°. This is larger than the 60–70 kcal/M of ΔH_{con}. A further striking difference between ΔH_d and ΔH_{con} is that ΔH_d is strongly temperature dependent while ΔH_{con} is not. The physical meaning of the temperature dependence of ΔH_d could be that the state of the denatured protein is constituted by an ensemble of many different interconverting steric structures which may have different energy parameters. Thus, a change of temperature will redistribute the populations of these different steric structures and lead to a change of the enthalpy difference, ΔH_d, with temperature. The fact that ΔH_{con} is independent of temperature indicates that the open states obtained by the fluctuations of the hydrogen exchange are not identical with the ensemble of states which constitute the thermally denatured protein.

(c) Partial unfolding

From the foregoing considerations it appears that the majority of the internal amide protons exchange by local unfolding mechanisms. To get an impression about the lower limit of the number of different internal motions which have to be assumed, the exchange rates at
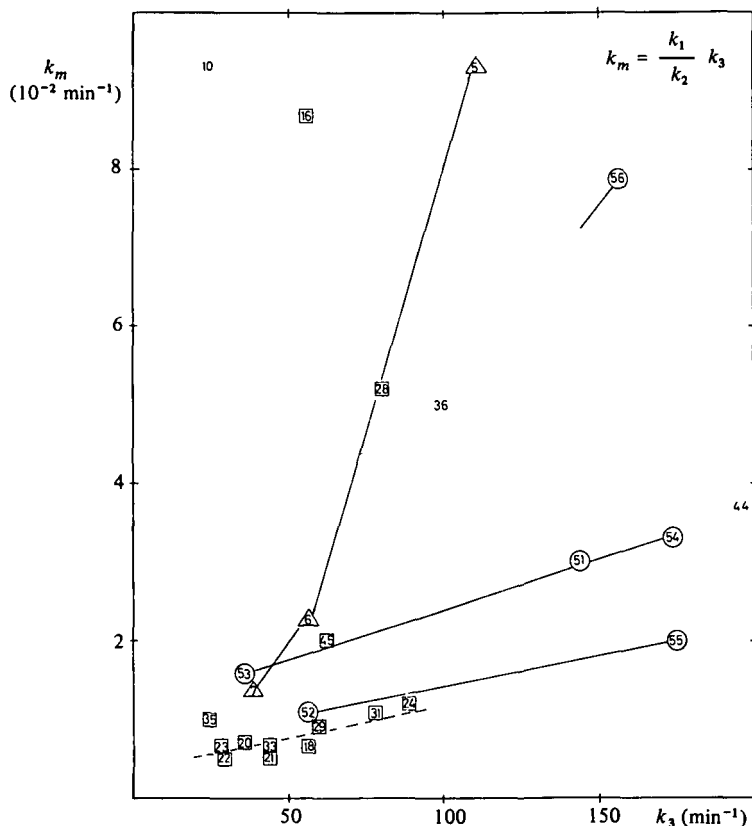
Fig. 9. Plot of the exchange rates, k_m, of the individual amide protons of BPTI *v.* their intrinsic exchange rates, k_3, at 68 °C, p^2H 3·5 (see Table 1). The data points are identified with the number in the amino acid sequence. Location in the β-sheet, the C-terminal α-helix and the N-terminal 3_{10}-helix is indicated by ($\square$), ($\bigcirc$) and ($\triangle$), respectively. In the domain of EX_2 exchange (equation 21), amide protons that get solvent contact only by the same fluctuation should appear on a straight line. Groups of protons of the same secondary structures for that such a correlation seems to be possible are connected in the figure. Six protons which exchange rather rapidly (Table 1) are not shown in the figure.

p^2H 3·5, 68°, of the individual amide protons were plotted in Fig. 9 *v.* the intrinsic exchange rate, k_3 (Table 1). Since we have EX_2-exchange at these conditions, the exchange rates of all amide protons that exchange due to the same internal motion should appear on a straight line, and the slope of this line would be the equilibrium constant, k_1/k_2 of the respective opening reaction (equation 21). Fig. 9 shows that the exchange in the N-terminal 3_{10}-helix could be explained by a single fluctuation. In the C-terminal α-helix at least three different fluctuations have to be assumed. In the central β-sheet

nine protons show a certain correlation with a correlation coefficient of 0·90 (Phe 22, Tyr 23, Arg 20, Tyr 21, Phe 33, Ile 18, Leu 29, Gln 31 and Asn 24). The spread of the data points around that straight line indicates the existence of several distinct, yet similar fluctuations. Additional fluctuations have to be assumed for the peripheral parts of the β-sheet (Tyr 35, Phe 45, Ala 16), and for the β-turn. The small-amplitude fluctuations of the β-sheet that are observed at very high p^{2}H have different characteristics: The exchange is slowest for the central strand of the triple stranded β-sheet (see Figs. 6, 7). These fluctuations could be interpreted as a rolling movement: when the three strands of the triple stranded β-sheet are represented by three parallel rods a rolling of the rods, where the topology of the molecule remains intact, would expose only the peptide protons of the outer rods. This could explain the slow exchange rates on the central strand.

(d) Correlation with protein stability

After the first measurements of the extremely slow exchange rates in BPTI two homologous proteins, the helix pomatia trypsin inhibitor and the cow colostrum trypsin inhibitor were studied (Wagner *et al.* 1978 *a,b*). The most striking observation was that the hydrogen exchange was much faster than in BPTI. This phenomenon could be correlated with the thermal stability. At certain conditions of p^{2}H and temperature (36°, p^{2}H 4·6), the exchange was faster the lower the denaturation temperature (Wagner & Wüthrich, 1979 *a*). This was first described only for amide protons of the β-sheet which have the most prominent spectral parameters. This statement also holds, however, for the α-helix, since in BPTI these protons exchange more slowly than all labile protons of helix pomatia trypsin inhibitor. Since a complete assignment of labile protons is only available for BPTI, a correlation with thermal stability could not be checked for the other labile protons. Later such a correlation was also found in chemically modified species of BPTI (Brown *et al.* 1978; Wagner, Tschesche & Wüthrich, 1979 *a*; Wagner, Kalb & Wüthrich, 1979 *b*; Wagner & Wüthrich, 1979 *a*; Wüthrich *et al.* 1980 *b*).

Woodward & co-workers (see Woodward & Hilton, 1980; Woodward *et al.* 1982) claim that this correlation between hydrogen exchange and thermal stability is valid only for the β-sheet region, and only in the range up to pH 8. They call this 'process A' and claim that it is cooperative unfolding of BPTI. The exchange at higher p^{2}H is called 'process B' which becomes dominant since process A has levelled out due to reaching the EX$_1$ limit (Woodward & Hilton, 1980).

These authors claim that only this process B describes mobility of the folded protein conformation and is not correlated with thermal stability. These statements have been checked by measurements in our laboratory. At first Wüthrich *et al.* (1980*b*) have studied a derivative of BPTI where the *S–S* bond 14–38 was reduced. In this molecule which is less stable against denaturation by heat than BPTI the hydrogen exchange is faster over the whole range from p²H 1 to p²H 10, even at the low temperature of 24°. The same observation was made when denaturing agents were used to reduce the thermal stability of BPTI (Roder, 1981). In the latter case it was further shown that at high p²H the small-amplitude fluctuations dominate the exchange, even above 50 °C (Roder *et al.*, manuscript in preparation). This indicates that the small amplitude fluctuations in the β-sheet are also correlated with the thermal stability.

Recently Hilton, Trudeau & Woodward (1981) have reported measurements of hydrogen–tritium exchange in BPTI, where the stability of the protein was reduced by adding urea. They find that at p²H 6·5 at 20–35 °C exchange is not correlated with the reduced stability. Measurements of single proton exchange rates, however, at the same conditions of temperature and p²H show positively such a correlation for protons of the β-sheet (Roder, 1981). This discrepancy seems to be due to the fact that Hilton *et al.* (1981) did not measure single proton exchange rates.

From a comparison of all these data it can be concluded that all the fluctuations which are relevant for hydrogen exchange in the β-sheet are generally related to the process of thermal unfolding but different from complete denaturation. This difference seems to be the size of the cooperative unit which may be either the β-sheet or the α-helix in internal fluctuations but not the whole protein as at the thermal unfolding. The small-amplitude fluctuations which are recorded at low temperature or high p²H appear to open only short fragments of the β-sheet. All these data were obtained only for a part of the buried amide protons. It may well be possible that there are molecular regions where fluctuations dominate isotope exchange which are independent of the thermal stability. Such a region might be the turn of the β-sheet but no data are available to decide on this question.

(*e*) *Comparison of molecular dynamics calculations*

The method of molecular dynamics calculations where the Newton equations of all the atoms of a protein are solved simultaneously (see

Karplus & McCammon, 1981 a) has become a powerful tool to study internal motions which occur on the psec time scale. Such motions may be manifested in NMR relaxation times. Levy, Karplus & McCammon (1981) claimed that these motions sizeably contribute to ^{13}C-relaxation times. Later Lipari & Szabo (1982) calculated the ^{13}C-relaxation times of the methyl groups of BPTI on the basis of molecular dynamics calculations and obtained a rather good fit of the experimental data of Richarz, Nagayama & Wüthrich (1980).

The internal motions which are responsible for hydrogen exchange occur on a much longer time scale. Nevertheless, Levitt (1981) has made an attempt to compare results of molecular dynamics calculations with hydrogen exchange data. He compared the experimental hydrogen exchange rates with the length of intramolecular hydrogen bonds, as obtained from the X-ray structure and from molecular dynamics calculations at two time periods (1–24 ps, 32–56 ps), and with the root-mean-square deviation of the hydrogen bond length from the mean value. He classified the intramolecular hydrogen bonds as stable or unstable according to the results of his calculations. This classification seemed to correlate well with the experimentally determined hydrogen exchange rates in a way that unstable or stable hydrogen bonds would belong to rapidly or slowly exchanging amide protons respectively. This comparison was biased by the uncompleteness of the set of exchange rates available at that time (Wüthrich & Wagner, 1979b). After the measurements of a complete set of exchange rates (Wagner & Wüthrich, 1982b) the correlation between the data of molecular dynamics calculations and the experimental hydrogen exchange rates is much worse. It appears therefore that the fast motions which can be simulated by molecular dynamics calculations are of little influence on the fluctuations which dominate the exchange of interior amide protons.

V. ROTATIONAL MOTIONS OF AROMATIC SIDE CHAINS

The exchange of labile backbone protons has provided some information on solvent exposure of the polypeptide backbone. The unique folding of a certain polypeptide to a globular conformation is a consequence of the primary structure; this means it is due to the sequence of amino acid side chains. In aqueous solution the majority of apolar groups tends to be in interior hydrophobic clusters while the polar groups of the backbone and the side chains which are located in the protein interior tend to form hydrogen bonds with other polar

groups. Among the most prominent hydrophobic side chains are the aromatic groups. In BPTI all interior aromatic side chains are located in essentially two hydrophobic clusters (Wüthrich *et al.* 1980*b*). In the crystal structure which gives a time averaged picture of the protein conformation, these aromatic side chains appear to be tightly packed between neighbouring groups. If these aromatic groups undergo rotational motions these neighbouring groups would move aside to allow for the rotational motions. Experimental observation of rotational motions thus gives information about the dynamics of the hydrophobic clusters in the protein interior.

(1) *Individual assignments*

BPTI contains four tyrosines and four phenylalanines as the only aromatic residues. The NMR resonances of the tyrosine side chains were first assigned by Snyder *et al.* (1975) by selective chemical modification. The spin systems of the phenylalanine rings were individually assigned by comparison of homologous and chemically modified proteins (Wagner *et al.* 1978*a, b*). Later on all the assignments of aromatic spin systems were confirmed by two-dimensional nuclear Overhauser effect spectroscopy (NOESY) without reference to the crystal structure (Wagner & Wüthrich, 1982*a*).

(2) *Detection of motions*

The rotational mobility of phenylalanine or tyrosine side chains in an anisotropic environment such as the protein interior is manifested by the symmetry of the spin system. A rotating tyrosine ring has a symmetric two-line spectrum of AA'BB' symmetry while a rigid side chain will generally show an unsymmetric four-line spectrum (Wüthrich & Wagner, 1979*a*). The transition from slow to fast rotation can be observed by variation of temperature (Wüthrich & Wagner, 1975; Campbell *et al.* 1976). In the transition range a quantitative determination of rotation rates is possible (Wagner, DeMarco & Wüthrich, 1976).

(3) 180° *flips*

The averaged resonances of the chemically equivalent ring protons are almost exactly in the middle of the resonance positions of the corresponding lines at low temperature. This is evidence that the averaging is only between two states, i.e. between two orientations of the ring corresponding to two indistinguishable energy minima. This means that the time spent in equilibrium orientation is long

TABLE 3. *Parameters for internal fluctuations of BPTI, calculated from the flipping motions of aromatic side chains*

Residue[*]	$\Delta G^{\ddagger}\ 40°$ (kcal M^{-1})		$\Delta H^{\ddagger}$ (kcal M^{-1})		$\Delta S^{\ddagger}$ (cal M^{-1} deg^{-1})		$\Delta V^{\ddagger}\ 56°$ (Å³)
	p²H 1·8	p²H 7·8	p²H 1·8	p²H 7·8	p²H 1·8	p²H 7·8	p²H 5·2
Tyr 23	—	14·7	—	26	—	35	—
Tyr 35	16·0	15·8	39	37	72	68	60
Phe 22	—	>20	—	—	—	—	—
Phe 45	13·8	13·7	16	17	6	11	50

[*] The flipping motions of Tyr 10, Tyr 21, Phe 4 and Phe 33 are too fast to be measured quantitatively by NMR.

compared with the time used for the flip motion. Otherwise the averaged resonance would not appear in the middle between the chemical shifts of the rigid ring. Thus ring flips are rare events compared with the lifetime of a particular ring orientation of minimum energy. With the information about 180° flips the spectra could be simulated and the flip rates were determined quantitatively at various temperature (Wagner *et al.* 1976), pressure (Wagner, 1980b) and pH (Wagner, 1982) values. The parameters obtained on the basis of transition state theory are summarized in Table 3.

(4) *Location of slowly rotating rings*

Of the eight aromatic side chains of BPTI five are in the slow rotational limit or in an intermediate situation somewhere in the temperature range between 4° and 80° (Wagner *et al.* 1976). The order of immobilization is: Phe 22, Tyr 35, Tyr 23, Phe 45 and Phe 33 (Wagner *et al.* 1976) with Phe 22 being the most immobilized one. To get information how strongly these side chains are buried in the protein interior, Table 4 lists the accessible surface areas of the heavy atoms of all aromatic side chains of BPTI as obtained from Dr C. Chothia (private communication, see Table 1). From these data it can be seen that all aromatic rings reach the protein surface, at least with one edge. The three rapidly rotating rings (Phe 4, Tyr 10, Tyr 21) appear to be more exposed to the solvent than the others.

(5) *Mechanism of ring rotation*

In the equilibrium conformation of BPTI rotational motions of the aromatic side chains are inhibited by very-high-energy barriers. Such motions are only possible if the energy barrier transiently decreases to a value in the order of thermal energy. The total activation energy

has thus two contributions: (i) the energy for the rearrangement of the protein conformation which allows the ring to flip; (ii) the residual repulsive interactions of the ring with its environment in the activated state. In addition fast collisional motions of the ring with its environment promote or dampen the flip process.

The forces acting on the aromatic ring have been separated in equation (9) in a static and a time dependent part. This separation is crucial since the potential $G(q)$ fluctuates also with time. It is reasonable to keep that part of $G(q)$, which fluctuates slowly compared with the intrinsic rotation rate, in the static part and to transfer fast fluctuations of $G(q)$ to the stochastic force $K(t)$. The question if the high or the low viscosity limit prevails is essentially a question if fast or slow fluctuations are dominant. To check on such arguments only a single flip rate can be measured in dependence of external parameters. Therefore simpler models have to be used which are capable to point out a few characteristic features of these motions which maybe checked on the experimental data.

(a) Opening model

The simplest description of the phenomenon is a two state model similar to that described by equation (18) for the hydrogen exchange. This implies that the environment of the ring opens to a certain extent so that the ring may flip over. Expressions like equations (19)–(21) are then obtained for the flip rate, k_m. The intrinsic flip rate is determined by the torsional potential of the aromatic side chain itself and by friction of the ring with its environment in the opened state. The torsional potential is very small (~ 0.5 kcal/M, see, for example, Momany *et al.* 1975) and can be neglected. The frictional effects are smaller the larger the opening of the environment. For large openings, an 'EX$_1$-type' process would result with a fast intrinsic flip movement where friction would not sizably decrease the intrinsic flip rate, k_3. For openings of small amplitude an 'EX$_2$-type' process would be obtained, with a rather slow intrinsic flip where friction would sizably reduce the intrinsic flip rate, k_3. k_3 is thus not independent of the amplitude of opening of the conformation. If there is a continuous distribution of fluctuations as indicated in Fig. 1 it has to be expected that the probe flips over mainly by openings of the smallest sufficient amplitude. In this case an EX$_2$-type mechanism would always dominate the rotational motion, and friction would play a considerable role.

Another possibility is that the distribution contains two discrete classes of fluctuations: small-amplitude fluctuations which never lead

to flips and large-amplitude fluctuations which always lead to a flip. In this case only an EX_1-type mechanism would occur.

This opening model which implies a distribution of open states has some parallels with Kramers' theory for rate processes. The EX_1-type mechanism would compare with the low viscosity limit where friction does not decrease the flip rate, while in the EX_2-type mechanism friction would sizably decrease the flip probability. Thus an EX_2 mechanism would be related to the high viscosity limit of Kramers' theory.

(b) Evaluation of data on the basis of Kramers' theory

Up to now only transition state theory was applied to evaluate experimental data on flip rates of internal aromatic rings in BPTI (Wagner et al. 1976; Wagner, 1980a). Use of Kramer's theory is difficult since no experimental information on internal viscosity in proteins is available.

Attempts have been made to use Kramers' theory for evaluation of other dynamic processes by Frauenfelder and co-workers (Beece et al. 1981). The point of their work is to keep the viscosity of the solution constant by adding different amounts of an inert viscous chemical while other parameters such as temperature or pressure are varied. The assumption made was that the relevant internal viscosity behaves parallel to the solvent viscosity. Thus real parameters of the activated process would be observed as long as the chemicals added are really inert to the protein. A similar attempt has been made in the case of BPTI to decide if low or high viscosity limits prevail for the flip motions of aromatic rings (Wagner & Eugster, to be published). Flip rates were measured at 50° with different amounts of ethylene glycol or glycerol added to increase solvent viscosity. The assumption was that internal viscosity is coupled to solvent viscosity in such a way that an increase of the solvent viscosity would either increase or at least not decrease the internal viscosity. Thus an increase or decrease of flip rates with solvent viscosity would indicate low viscosity limit or high viscosity limit, respectively. The experiments carried out at 50° showed a significant increase of flip rates, by a factor of $\sim 1\cdot5$, when 57 % ethylene glycol was added. This would indicate the low viscosity limit as long as ethylene glycol was inert to the protein. To check the latter point the denaturation temperature was measured in the presence and absence of 57 % ethylene glycol and was found to be 7° lower in the presence of the chemical. As a cross-check the chemically related ethanol was used which is known to have a much

stronger effect on the protein stability than ethylene glycol (von Hippel & Wong, 1965) while only slightly changing the viscosity (Landolt-Börnstein, 1969). In this case a much stronger increase of flip rates was observed. This indicates that the increase of flip rates by ethylene glycol may not be a viscosity effect but a destabilizing effect of a non-inert chemical (Wagner & Eugster, to be published). It is therefore further in question if low or high viscosity limit prevail for the rotational motions of internal aromatic side chains.

Karplus & McCammon (1981 b) claim that for these processes the viscosity is in an intermediate situation or in the high damping limit. This assumption is based on results of computer calculations where the aromatic ring of Tyr 35 is turned by 90° and subsequently allowed to swing back to its original orientation (McCammon & Karplus, 1979, 1980). Unfortunately no experiments are available to check on these arguments.

(c) Significance of kinetic parameters

For the evaluation of the data about ring flips transition state theory must thus be applied. However, it would be of interest to consider how strongly parameters such as activation enthalpy or activation volume might change when Kramers' theory could be applied. To get such estimates assumptions have to be made about the viscosity in the interior of globular proteins. Assuming this viscosity behaves similar to that of normal liquid hydrocarbons (Karplus & McCammon, 1981 b) we have

$$\left(\frac{\partial \ln \eta}{\partial p}\right)_{T = 25_0} \cong 8 \times 10^{-4} \text{ atm}^{-1}, \tag{27}$$

and

$$\left(\frac{\partial \ln \eta}{\partial 1/T}\right)_{p = 1 \text{ bar}} \cong 800 \text{ deg} \quad \text{(Landolt-Börnstein, 1969)}. \tag{28}$$

This would add or subtract ~ 35 Å^3 to the activation volumes determined on the basis of transition state theory. (See equations 14–17.)

Thus for interpretation of activation volumes frictional effects may be crucial. The temperature dependence of the viscosity is negligibly small compared to the temperature dependence of the rates of ring flips and thus activation enthalpies can be determined without information about internal frictional effects.

(6) *Computer simulations of ring flips in BPTI*

The detailed experimental information on ring flips in BPTI has stimulated a number of theoretical studies on this problem. At first Gelin & Karplus (1975) calculated the energy of the protein while rotating the tyrosine side chains in small steps about the C^β-C^γ-axis. The maximum of energy was obtained when the ring was approximately perpendicular to the equilibrium orientation and should be compared with the activation enthalpy obtained from the experiments. When the surrounding protein matrix was kept rigid for any orientation of the aromatic ring the energy barriers calculated were very high compared with the experimental activation enthalpies. However, when flexibility was included the protein matrix was allowed to relax at each orientation of the rotated ring, energy barriers were obtained which were of the right order of magnitude but a factor $\sim$ o·5 to low. Hetzel *et al.* (1976) made a similar approach using different energy functions. They also obtained very-high-energy barriers for the rigid conformation and values with the right order of magnitude when the protein was allowed to relax. These authors further calculated an alternative model where the aromatic ring was replaced by a sphere which had a volume similar to that occupied by a freely rotating ring. The calculated energy barriers were again in the right order of magnitude when the protein was allowed to relax although the energies were slightly higher than the experimental values of the activation enthalpies. Hetzel *et al.* (1976) thus treated two models which are analogous to the low viscosity limit (the 'free volume' model) where little contact of the rotating ring exists with its environment, and the high viscosity limit where close contact of ring and matrix is allowed continuously during the rotational motion. Considering that these calculations all give the right order of magnitude but not the correct rank order for the different aromatic side chains, these calculations should not be used to discard either model. It should also be kept in mind that all these calculations neglected the solvent, which may be crucial because one edge of each internal aromatic side chain of BPTI reaches the protein surface (see Table 4).

To get further insight into the dynamics of ring flips McCammon & Karplus (1979, 1980) used a more detailed method. They took a set of coordinates from an equilibrium dynamical simulation of BPTI. Then the ring of Tyr 35 was rigidly rotated to a high energy orientation. Subsequently the protein was allowed to relax by Monte Carlo methods (Metropolis *et al.* 1953) while the ring was held fixed.

TABLE 4. *Accessible surface area of the heavy atoms of the aromatic side chains in $\mathring{A}^2$ as defined by Lee & Richards* (1971)

(The data were kindly given to us by Dr Chothia (see Table 1). The two rows for the C^δ and C^ϵ atoms correspond to the two edges of the rings.)

Residue	C^γ	C^δ	C^ϵ	C^ξ	O^η	Total
Phe 4	0·0	$\left\{\begin{array}{l}0\cdot0\\11\cdot2\end{array}\right.$	$\left.\begin{array}{l}0\cdot6\\6\cdot0\end{array}\right\}$	6·1	—	23·9
Tyr 10	0·0	$\left\{\begin{array}{l}15\cdot1\\0\cdot0\end{array}\right.$	$\left.\begin{array}{l}24\cdot9\\2\cdot2\end{array}\right\}$	5·4	29·4	77·0
Tyr 21	0·0	$\left\{\begin{array}{l}0\cdot0\\0\cdot0\end{array}\right.$	$\left.\begin{array}{l}10\cdot6\\1\cdot0\end{array}\right\}$	0·7	28·0	40·3
Phe 22	0·0	$\left\{\begin{array}{l}0\cdot3\\0\cdot0\end{array}\right.$	$\left.\begin{array}{l}6\cdot0\\5\cdot2\end{array}\right\}$	10·5	—	22·0
Tyr 23	0·0	$\left\{\begin{array}{l}0\cdot0\\0\cdot0\end{array}\right.$	$\left.\begin{array}{l}3\cdot8\\0\cdot0\end{array}\right\}$	0·8	2·5	7·1
Phe 33	0·0	$\left\{\begin{array}{l}0\cdot8\\0\cdot0\end{array}\right.$	$\left.\begin{array}{l}0\cdot0\\0\cdot0\end{array}\right\}$	0·4	—	1·2
Tyr 35	0·0	$\left\{\begin{array}{l}0\cdot0\\0\cdot0\end{array}\right.$	$\left.\begin{array}{l}0\cdot0\\6\cdot8\end{array}\right\}$	0·0	6·2	13·0
Phe 45	0·0	$\left\{\begin{array}{l}0\cdot0\\9\cdot0\end{array}\right.$	$\left.\begin{array}{l}0\cdot0\\11\cdot8\end{array}\right\}$	0·0	—	20·8

After some further relaxation steps and repeated sampling they claimed to have an ensemble of states representative for the transition state. For computing trajectories which pass through a given configuration of the transition state, velocities were assigned to the ring in the activated state. The subsequent 'falling down' from the activated to the equilibrium state was simulated by molecular dynamics calculations (McCammon & Karplus, 1979). The 'falling down' the other side of the barrier was taken as the process of reaching the activated state with inverted time (see Karplus & McCammon, 1981 a). The crucial part of these calculations is the construction of the activated state. Since these authors let the protein matrix relax after the ring was rotated by 90° they impicitely assumed the high damping limit from the very beginning. Thus, results of these calculations cannot be used to corroborate the high viscosity limit assumption. It would be very interesting to have computer simulations of the path from the equilibrium conformation to the activated state with the right time direction. From such calculations highly relevant information about this intramolecular process could be obtained.
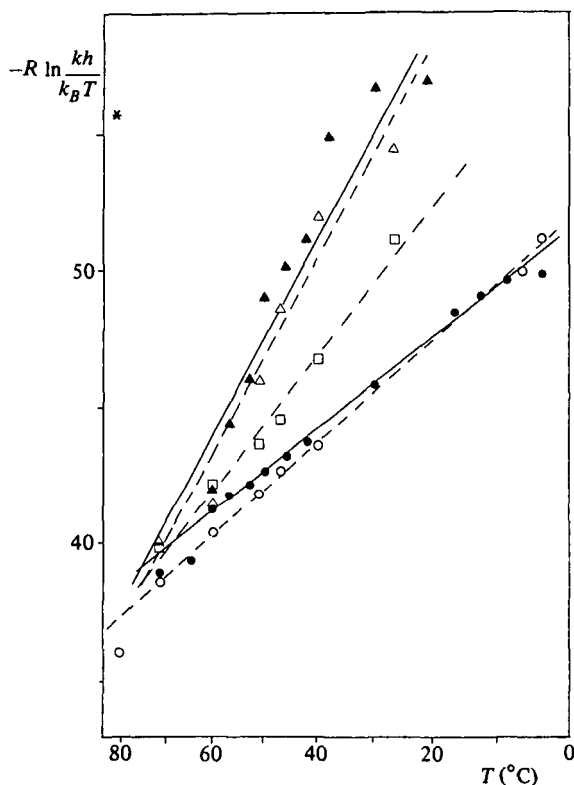
Fig. 10. Eyring plots for the flip rates, k, of the aromatic rings of Tyr 23 ($\square$), Tyr 35 ($\triangle$, $\blacktriangle$) and Phe 45 ($\bigcirc$, $\bullet$). Open symbols represent the data obtained at p^2H 7·8, full symbols those at p^2H 1·8. $*$ represents a single measurement on the immobilized Phe 22 at 81°, p^2H 7·8. $-R \ln (kh/k_BT)$ (in kcal/mol·deg) is plotted $v. 1/T$. (Reproduced from Wagner, 1982.)

(7) *Change of experimental conditions*

Variation of temperature, pressure, pH or solvent may change the distribution of fluctuations which are seen by the flipping aromatic side chains.

(a) *Variation of temperature*

For three aromatic side chains of BPTI the effect of temperature on flip rates has been measured (Wagner *et al.* 1976; Wagner, 1982). The results are shown in Fig. 10 in an Eyring plot representation. Within the experimental accuracy these plots do not show a deviation from linearity. Thus from this observation no redistribution of protein fluctuations with temperature can be concluded.

As a second check on a redistribution of fluctuations the effect of

some chemicals was tested (Wagner & Eugster, to be published). Ethanol significantly accelerates ring flips at 50° but has no effect at 24°. Similar but smaller effects have been observed with ethylene glycol and glycerol. These results indicate that at the higher temperature fluctuations which can be influenced by chemicals like ethanol are important and are not present at the lower temperature. Since it is assumed that, in protein solutions, ethanol acts mainly on the water structure (von Hippel & Wong, 1965), it appears that the fluctuations at high temperature involve an increased water access to the hydrophobic clusters which contain the internal aromatic rings in BPTI.

(b) *Variation of pressure*

In contrast to the pressure dependence of NH exchange (see Fig. 6) the logarithm of the flip rates *v.* pressure shows rather straight lines at least up to the highest pressures measured (Wagner, 1980*a*; 1982). This gives no indication for a change of the distribution of fluctuations with pressure. No further tests have been performed to study if such a redistribution of fluctuations occurs with pressure.

The pressure dependence of the flip rates has first been interpreted on the basis of transition state theory (Wagner, 1980*a*). Later it has been pointed out that a use of Kramers' theory would modify the size of the activation volumes derived (Karplus & McCammon, 1981*b*; Wagner, 1982). In the case of the low viscosity limit the activation volumes might be as large as 90° $Å^3$ while for the high viscosity limit the values might become as small as 20–30 $Å^3$. Also these values, however, would well account for the volume of neighbouring groups which are located in the rotation sphere according to the crystal structure and would have to move aside for a frictionless flip (Wagner, 1980*a*, 1982). We therefore favour the free volume model interpretation for these internal motions.

(c) *Variation of charge distribution*

Flip rates of Phe 45 and Tyr 35 were measured at pH 7·8 and 1·8 at various temperatures (see Fig. 10). Within the experimental accuracy the results are identical for both pH values. Phe 45 is close in space to Asp 50, the side chain of which forms a hydrogen bond to the peptide NH of Lys 46 above pH 3. Nevertheless the mobility of this aromatic side chain is unaffected by the titration of Asp 50 and all other carboxylic acid side chains. Thus opening and reforming of hydrogen bonds and salt bridges appears to be without effect on the internal motions which are recorded by the flipping aromatic side

chains as long as the gross spatial structure of the protein is unchanged.

Similar information is obtained when homologous proteins are studied. In the two trypsin inhibitors of cow colostrum and *helix pomatia* very few ionizable groups are at homologous positions (Wagner *et al.* 1978*b*). Nevertheless, the homologous internal aromatic side chains show very similar dynamic behaviour in the three proteins.

(*d*) *Local modifications of the protein*

Several chemically modified derivatives of BPTI were investigated by NMR. Only such derivatives were further studied where the gross conformation was maintained. These modifications are: cleavage of the *S-S*-bond 14–38 (Wagner *et al.* 1979*a, b*), cleavage of the peptide bond Lys 15–Ala 16, removal of Ala 16 and Arg 17 (Wagner *et al.* 1979*a*), and transamination of the amino terminus (Brown *et al.* 1978). The mobility of Phe 45, a residue which is distant from all these modification sites was only slightly influenced by these modifications. Tyr 35 is spatially close to the *S-S*-bond 14–38 and the backbone strand Lys 15 to Arg 17. The modifications at these sites strongly influenced the mobility of Tyr 35. Transamination of the N-terminus somehow affects the conformation around the side chain of Tyr 23. As a consequence the dynamic behaviour of this side chain also appears to be affected (Brown *et al.* 1978). These experiments indicate that the fluctuations reported by flipping aromatic side chains are local processes within hydrophobic clusters of the protein interior.

(8) *Mechanistic Aspects*

Besides the different flip rates at high and low temperature, the nature of the structural fluctuations, recorded by the ring flips, may be different at the two extreme conditions. This is indicated by the different influence of chemicals at low and high temperature. Thus a general picture of the fluctuation, which governs the flips, can not be given. Nevertheless, the general features may be discussed. There are two alternative models: the first model favours the high viscosity limit. In this model frequent collisions would occur between the ring and its environment during the flipping motion. These collisions should drive the ring over the barrier and dampen the initialized motion. A successful flip would thus require a number of subsequent promoting collisions or an exceedingly strong initial promoting collision, much stronger than the many subsequent opposing col-

lisions. From the kind of figures shown by McCammon & Karplus (1980) this appears to be unlikely. It seems that a ring would never flip over with this kind of damping collisions unless the particles do not collide for a short time after the flipping motion has been initialized. This is the assumption of the second model which has been called a 'free volume' model (Hetzel *et al.* 1976; Wagner, 1980*b*, 1982; Karplus & McCammon, 1981 *a*). Every protein structure also has some packing defects, close to internal aromatic side chains. These free volume chambers may fluctuate in size. The volume work necessary to open a free volume of 100 Å^3 is in the order of 1·4 cal M^{-1}. Thus this process may be possible. Assuming the low viscosity limit with corrections for the pressure dependence of the viscosity, the activation volumes determined for the flipping motions of Tyr 35 and Phe 45 (Wagner, 1980*b*; 1982) would almost exactly fit the volume of the sphere used in the model calculations of Hetzel *et al.* (1976).

VI. SUMMARY

The experimental observations described in this article indicated that a distribution of many different fluctuations is present in a globular protein. These fluctuations were characterized by observation of many natural internal probes such as the labile peptide protons and the aromatic side chains. The conditions which are necessary to get reactions of the internal probes have been discussed in detail. The structural interpretation of the data was facilitated by the development and the use of new NMR techniques which provided the identification of the resonances of all the labile peptide protons. With NOE measurements a distinction between correlated and uncorrelated exchange events was obtained. This enabled us to elucidate the exchange mechanism over a wide range of p^2H and temperature and to classify different subsets of fluctuations with respect to their lifetimes. It was further demonstrated that a change of external conditions such as temperature, p^2H or pressure can change the distribution of fluctuations in the protein. The mechanisms responsible for rotation of internal aromatic side chains were also found to change with temperature, and mechanistic aspects of these fluctuations were discussed.

This demonstration of a manifold of spatial fluctuations in a small protein provides an impression on the kind of fluctuations which have to be expected for larger proteins. When studying protein reactions one should therefore consider the presence of a large number of

different, transiently formed, spatial structures available for the partner in the reaction, which may pick out only that structure which will optimally perform a particular reaction with the highest efficiency.

VII. REFERENCES

ARTYMIUK, P. J., BLAKE, C. C. F., GRACE, D. E. P., OATLEY, S. J., PHILLIPS, D. C. & STERNBERG, M. J. E. (1979). Crystallographic studies of the dynamic properties of lysozyme. *Nature, Lond.*, **280**, 563–568.

AUSTIN, R. H., BEESON, K. W., EISENSTEIN, L., FRAUENFELDER, H. & GUNSALUS, I. C. (1975). Dynamics of ligand binding to myoglobin. *Biochemistry, Philad.* **14**, 5355–5373.

BEECE, D., EISENSTEIN, L., FRAUENFELDER, H., GOOD, D., MARDEN, M. C., REINISCH, L., REYNOLDS, A. H., SORENSEN, L. B. & YUE, K. T. (1981). Solvent viscosity and protein dynamics. *Biochemistry, Philad.* **19**, 5147–5157.

BROWN, L. R., DeMARCO, A., RICHARZ, R., WAGNER, G. & WÜTHRICH, K. (1978). The influence of a single salt bridge on the static and dynamic features of the globular solution conformation of the basic pancreatic trypsin inhibitor: ^{1}H and ^{13}C NMR studies of the native and the transaminated inhibitor. *Eur. J. Biochem.* **88**, 87–95.

CAMPBELL, I. D., DOBSON, C. M., MOORE, G. R., PERKINS, S. J. & WILLIAMS, R. J. P. (1976). Temperature dependent molecular motions of a tyrosine residue of ferrocytochrome *c*. *FEBS Lett.* **70**, 96–100.

CARERI, G., FASELLA, P. & GRATTON, E. (1975). Statistical time events in enzymes: a physical assessment. *CRC Crit. Rev. Biochem.* **3**, 141–164.

CARTER, J. V., KNOX, D. G. & ROSENBERG, A. (1978). Pressure effects on folded proteins in solution. *J. biol. Chem.* **253**, 1947–1953.

CHOTHIA, C. & JANIN, J. (1975). Principles of protein–protein recognition. *Nature, Lond.* **256**, 705–708.

COOPER, A. (1976). Thermodynamic fluctuations in protein molecules. *Proc. natn. Acad. Sci. U.S.A.* **73**, 2740–2741.

CREIGHTON, T. E. (1978). Experimental studies of protein folding and unfolding. *Prog. Biophys. Molec. Biol.* **33**, 231–297.

DEISENHOFER, J. & STEIGEMANN, W. (1975). Crystallographic refinement of the structure of bovine pancreatic trypsin inhibitor at 1·5 Å resolution. *Acta crystallogr.* **B31**, 238–250.

DUBS, A., WAGNER, G. & WÜTHRICH, K. (1979). Individual assignments of amide proton resonances in the proton NMR spectrum of the basic pancreatic trypsin inhibitor. *Biochim. biophys. Acta.* **577**, 177–194.

EIGEN, M. (1964). Proton transfer, acid-base catalysis, and enzymatic hydrolysis. *Angew. Chem.* **3**, 1–19.

ENGLANDER, S. W. & POULSEN, A. (1969). Hydrogen–tritium exchange of the random chain polypeptide. *Biopolymers* **7**, 379–393.

ENGLANDER, S. W., DOWNER, S. W. & TEITELBAUM, H. (1972). Hydrogen exchange. *A. Rev. Biochem.* **41**, 903–924.

EYRING, H. (1935). The activated complex in chemical reactions. *J. chem. Phys.* **3**, 107–115.

FRAUENFELDER, H., PETSKO, G. A. & TSERNOGLOU, D. (1979). Temperature-dependent X-ray diffraction as a probe of protein structural dynamics. *Nature, Lond.* **280**, 558–563.

GROTE, R. F. & HYNES, J. T. (1980). The stable state picture of chemical reactions. II. Rate constants for condensed and gas phase reaction models. *J. chem. Phys.* **73**, 2715–2732.

GURD, F. R. N. & ROTHGEB, T. M. (1979). Motions in proteins. *Adv. Protein Chem.* **33**, 73–165.

HETZEL, R., WÜTHRICH, K., DEISENHOFER, J. & HUBER, R. (1976). Dynamics of the basic pancreatic trypsin inhibitor (BPTI). II. Semi-empirical energy calculations. *Biophys. Struct. & Mechanism* **2**, 159–180.

HILTON, B. D. & WOODWARD, C. K. (1979). On the mechanism of isotope exchange kinetics of single protons in bovine pancreatic trypsin inhibitor. *Biochemistry, Philad.* **18**, 5834–5841.

HILTON, B. D., TRUDEAU, K. & WOODWARD, C. K. (1981). Hydrogen exchange rates in pancreatic trypsin inhibitor are not correlated to thermal stability in urea. *Biochemistry, Philad.* **20**, 4697–4703.

HUBER, R. L. (1979). Conformational flexibility and its functional significance in some protein molecules. *Trends Biochem. Sci.* **4**, 271–276.

HVIDT, A. & NIELSEN, S. O. (1966). Hydrogen exchange in proteins. *Adv. Protein Chem.* **21**, 287–386.

JULLIEN, M. & BALDWIN, R. L. (1981). The role of proline residues in the folding kinetics of the bovine pancreatic trypsin inhibitor derivative RCAM (14–38). *J. molec. Biol.* **145**, 265–280.

KARPLUS, M. & McCAMMON, J. A. (1980). Dynamics of tyrosine ring rotations in a globular protein. *Biopolymers* **19**, 1375–1405.

KARPLUS, M. & McCAMMON, J. A. (1981a). The internal dynamics of globular proteins. *C.R.C. Crit. Rev. Biochem.* **9**, 293–349.

KARPLUS, M. & McCAMMON, J. A. (1981b). Pressure dependence of aromatic ring rotations in proteins: a collisional interpretation. *FEBS Lett.* **131**, 34–36.

KOSSIAKOFF, A. A. (1982). Protein dynamics investigated by the neutron

diffraction hydrogen exchange technique. *Nature, Lond.* **296**, 713–721.

KRAMERS, H. A. (1940). Brownian motion in a field of force and the diffusion model of chemical reactions. *Physica* **7**, 285–304.

KUBO, R. (1966). The fluctuation–dissipation theorem. *Rep. Prog. Phys.* **29**, 255–284.

LANDOLT-BÖRNSTEIN (1969). *Zahlenwerte und Funktionen, Transportphänomene*, vol. 1. Berlin: Springer Verlag.

LEE, B. & RICHARDS, F. M. (1971). The interpretation of protein structures: Estimation of static accessibility. *J. molec. Biol.* **55**, 379–400.

LEVITT, M. (1981). Molecular dynamics of hydrogen bonds in bovine pancreatic trypsin inhibitor protein. *Nature, Lond.* **294**, 379–380.

LEVY, R. M., KARPLUS, M. & McCAMMON, J. A. (1981). Increase of ^{13}C NMR relaxation times in proteins due to picosecond motional averaging. *J. Am. chem. Soc.* **94**, 2657–2660.

LUMRY, R. & ROSENBERG, A. (1975). The mobile defect hypothesis of protein function. *Coll. Int. C.N.R.S. L'Eau. Syst. Biol.* **246**, 55–63.

LIPARI, G. & SZABO, A. (1982). Model-free approach to the interpretation of nuclear magnetic resonance relaxation in macromolecules. 2. Analysis of experimental results. *J. Am. Chem. Soc.* **104**, 4559–4570.

MARINETTI, T. D., SNYDER, G. H. & SYKES, B. D. (1976). Nuclear magnetic resonance determination of intramolecular distances in bovine pancreatic trypsin inhibitor using nitrotyrosine chelation of lanthanides. *Biochemistry, Philad.* **15**, 4600–4608.

MASSON, A. & WÜTHRICH, K. (1973). Proton magnetic resonance investigation of the conformational properties of the basic pancreatic trypsin inhibitor. *FEBS Lett.* **31**, 114–118.

McCAMMON, J. A. & KARPLUS, M. (1979). Dynamics of activated processes in globular proteins. *Proc. natn. Acad. Sci. U.S.A.* **76**, 3585–3589.

McCAMMON, J. A. & KARPLUS, M. (1980). Dynamics of tyrosine ring rotations in a globular protein. *Biopolymers* **19**, 1375–1405.

METROPOLIS, N., ROSENBLUTH, A. W., ROSENBLUTH, M. N., TELLER, A. H. & TELLER, E. (1953). Equation of state calculations by fast computing machines. *J. chem. Phys.* **21**, 1087–1092.

MOLDAY, R. S., ENGLANDER, S. W. & KALLEN, R. G. (1972). Primary structure effects on peptide group hydrogen exchange. *Biochemistry, Philad.* **11**, 150–158.

MOMANY, F. A., McGUIRE, R. F., BURGES, A. W. & SCHERAGA, H. A. (1975). Energy parameters in polypeptides. VII. Geometric parameters, partial atomic charges, non bonded interactions and intrinsic torsional potential for naturally occuring amino acids. *J. phys. Chem.* **79**, 2361–2381.

NAGAYAMA, K. & WÜTHRICH, K. (1981). Systematic application of two-dimensional ^{1}H nuclear-magnetic-resonance techniques for studies of proteins. 1. combined use of spin-echo-correlated spectroscopy and J-resolved spectroscopy for the identification of complete spin

systems of non-labile protons in amino-acid residues. *Eur. J. Biochem.* **114**, 369–374.

PELZER, H. & WIGNER, E. (1932). Ueber die Geschwindigkeitskonstante von Austauschreaktionen. *Z. phys. Chem. B* **15**, 445–471.

POHL, F. M. (1976). Temperature-dependence of the kinetics of folding of chymotrypsinogen A. *FEBS Lett.* **65**, 293–296.

PRIVALOV, P. L. (1979). Stability of proteins. Small globular proteins. *Adv. Protein Chem.* **33**, 167–241.

RICHARDS, F. M. (1977). Areas, volumes, packing, and protein structure. *Ann. Rev. Biophys. Bioengng.* **6**, 151–176.

RICHARDS, F. M. (1979). Packing defects, cavities, volume fluctuations, and access to the interior of proteins. Including some general comments on surface area and protein structure. *Carlsberg Res. Commun.* **44**, 47–63.

RICHARZ, R., SEHR, P., WAGNER, G. & WÜTHRICH, K. (1979). Kinetics of the exchange of individual amide protons in the basic pancreatic trypsin inhibitor. *J. molec. Biol.* **130**, 19–30.

RICHARZ, R., NAGAYAMA, K. & WÜTHRICH, K. (1980). Carbon-13 nuclear magnetic resonance relaxation studies of internal mobility of the polypeptide chain in basic pancreatic trypsin inhibitor and a selectively reduced analogue. *Biochemistry, Philad.* **19**, 5189–5196.

RODER, H. (1981). Interne Mobilität in Proteinen unter nativen und denaturierenden Bedingungen: Untersuchung von Trypsin-Inhibitoren mit spektroskopischen Methoden. Ph.D. Thesis Nr. 6932, ETH Zürich.

ROSA, J. J. & RICHARDS, F. M. (1979). An experimental procedure of increasing the structural resolution of chemical hydrogen-exchange measurements on proteins: applications to ribonuclease S peptide. *J. molec. Biol.* **133**, 399–416.

SNYDER, G. H., ROWAN, R., KARPLUS, S. & SYKES, B. D. (1975). Complete tyrosine assignments in the high field ^{1}H nuclear magnetic resonance spectrum of the bovine pancreatic trypsin inhibitor. *Biochemistry, Philad.* **14**, 3765–3777.

SKINNER, J. L. & WOLYNES, P. G. (1978). Relaxation processes and chemical kinetics. *J. chem. Phys.* **69**, 2143–2150.

VINCENT, J. P., CHICHEPORTICHE, R. & LAZDUNSKI, M. (1971). The conformational properties of the basic pancreatic trypsin inhibitor. *Eur. J. Biochem.* **23**, 401–411.

TÜCHSEN, E., HVIDT, A. & OTTESEN, M. (1980). Enzymes immobilyzed as crystals. Hydrogen exchange of crystalline lysozyme. *Biochimie* **62**, 563–566.

VON HIPPEL, P. H. & WONG, K.-Y. (1965). On the conformational mobility of globular proteins. *J. biol. Chem.* **240**, 3909–3923.

WAGNER, G. (1980 a). Activation volumes for the rotational motion of interior aromatic rings in globular proteins determined by high resolution ^{1}H NMR at variable pressure. *FEBS Lett.* **112**, 280–284.

WAGNER, G. (1980 *b*). A novel application of Nuclear Overhauser Enhancement (NOE) in proteins: analysis of correlated events in the exchange of internal labile protons. *Biochem. biophys. Res. Commun.* **97**, 614–620.

WAGNER, G. (1982). Internal mobility in globular proteins. *Comments Mol. Cell. Biophys.* **1**, 261–280.

WAGNER, G. & WÜTHRICH, K. (1979 *a*). Correlation between the amide proton exchange rates and the denaturation temperature in globular proteins related to the basic pancreatic trypsin inhibitor. *J. molec. Biol.* **130**, 31–37.

WAGNER, G. & WÜTHRICH, K. (1979 *b*). Structural interpretation of the amide proton exchange in the basic pancreatic trypsin inhibitor and related proteins. *J. molec. Biol.* **134**, 75–94.

WAGNER, G. & WÜTHRICH, K. (1982 *a*). Sequential resonance assignments in protein ^{1}H NMR spectra: basic pancreatic trypsin inhibitor. *J. molec. Biol.* **155**, 347–366.

WAGNER, G. & WÜTHRICH, K. (1982 *b*). Amide proton exchange and surface conformation of the basic pancreatic trypsin inhibitor (BPTI) in solution: studies with two-dimensional nuclear magnetic resonance. *J. molec. Biol.* **160**, 343–361.

WAGNER, G., DeMARCO, A. & WÜTHRICH, K. (1976). Dynamics of the aromatic amino acid residues in the globular conformation of the basic pancreatic trypsin inhibitor (BPTI). I. ^{1}H NMR studies. *Biophys. struct. & Mechanism* **2**, 139–158.

WAGNER, G., WÜTHRICH, K. & TSCHESCHE, H. (1978 *a*). A ^{1}H NMR study of the conformation and the molecular dynamics of the glycoprotein cow colostrum trypsin inhibitor. *Eur. J. Biochem.* **86**, 67–76.

WAGNER, G., WÜTHRICH, K. & TSCHESCHE, H. (1978 *b*). A ^{1}H NMR study of the solution conformation of the isoinhibitor K from Helix pomatia. *Eur. J. Biochem.* **89**, 367–377.

WAGNER, G., TSCHESCHE, H. & WÜTHRICH, K. (1979 *a*). The influence of a localized chemical modification of the basic pancreatic trypsin inhibitor on static and dynamic aspects of the molecular conformation in solution. *Eur. J. Biochem.* **95**, 239–248.

WAGNER, G., KALB, A. J. & WÜTHRICH, K. (1979 *b*). Conformational studies by ^{1}H NMR of the basic pancreatic trypsin inhibitor after reduction of the disulfide bond 14–38. Influence of charge protecting groups on the stability of the protein. *Eur. J. Biochem.* **95**, 249–253.

WAGNER, G., ANIL KUMAR & WÜTHRICH, K. (1981). Systematic application of two-dimensional ^{1}H NMR techniques for studies, of proteins. 2. Combined use of correlated spectroscopy and nuclear Overhauser spectroscopy for sequential assignments of· backbone resonances and elucidation of polypeptide secondary structures. *Eur. J. Biochem.* **114**, 375–384.

WLODAWER, A. & SJÖLIN, L. (1982). Hydrogen exchange in RNase A: Neutron diffraction study. *Proc. natn. Acad. Sci. U.S.A.* **79**, 1418–1422.

WOODWARD, C. K. & HILTON, B. D. (1980). Hydrogen isotope exchange

kinetics of single protons in bovine pancreatic trypsin inhibitor. *Biophys. J.* **32**, 561–575.

WOODWARD, C., SIMON, I. & TÜCHSEN, E. (1982). Hydrogen exchange and the dynamic structure of proteins. *Mol. & Cell. Biochem.* (in press).

WÜTHRICH, K. (1976). *Nuclear Magnetic Resonance in Biological Research – Peptides and Proteins*, Amsterdam: North-Holland.

WÜTHRICH, K. & WAGNER, G. (1975). NMR investigations of the dynamics of the aromatic amino acid residues in the basic pancreatic trypsin inhibitor. *FEBS Lett.* **50**, 265–268.

WÜTHRICH, K. & WAGNER, G. (1979a). Internal motions in globular proteins. *Trends Biochem. Sci.* **3**, 227–230.

WÜTHRICH, K. & WAGNER, G. (1979b). Nuclear magnetic resonance of labile protons in the basic pancreatic trypsin inhibitor. *J. molec. Biol.* **130**, 1–18.

WÜTHRICH, K. & WAGNER, G. (1982). NMR studies of concerted motions in the interior and on the surface of globular proteins. Proc. *Ciba Fdn. Symp. on Internal Motions in Proteins*, *London* (in the press).

WÜTHRICH, K., EUGSTER, A. & WAGNER, G. (1980a). p^{2}H dependence of the exchange with the solvent of interior amide protons in basic pancreatic trypsin inhibitor modified by reduction of the disulfide bond 14–38. *J. molec. Biol.* **144**, 601–604.

WÜTHRICH, K., WAGNER, G., RICHARZ, R. & BRAUN, W. (1980b). Correlation between internal mobility and stability of globular proteins. *Biophys. J.* **32**, 549–560.